Development of a New Packing Element for Packed Bed Absorber

by

Muhammad Aiman bin Sapree

SID: 13198

Dissertation submitted in partial fulfilment of

the requirements for the

Bachelor of Engineering (Hons)

(Chemical Engineering)

JANUARY 2014

Universiti Teknologi PETRONAS

Bandar Seri Iskandar

31750 Tronoh

Perak Darul Ridzuan

CERTIFICATION OF APPROVAL

Development of a New Packing Element for Packed Bed Absorber

by

Muhammad Aiman bin Sapree

A project dissertation submitted to the

Chemical Engineering Department

Universiti Teknologi PETRONAS

in partial fulfillment of the requirement for the

BACHELOR OF ENGINEERING (Hons)

(CHEMICAL ENGINEERING)

Approved:

…………………………..
(Prof Dr Duvvuri Subbarao)

UNIVERSITI TEKNOLOGI PETRONAS

TRONOH, PERAK

January 2014

i

CERTIFICATION OF ORIGINALITY

I hereby certify that I am responsible for the work submitted in this project, that the original work is my own except as specified in the references and acknowledgements, and that the original work contained herein have not been undertaken or done by unspecified sources or persons to the extent of my knowledge and information.

....

(MUHAMMAD AIMAN BIN SAPREE)

ABSTRACT

Packed towers are commonly used in separation processes such as absorption, extraction, distillation, and stripping. Packed towers contain packing element which improve contact between the two contacting phase. The development of the packing elements has been extensive since its first introduction in the industry. The previous generations of packing element are made of rigid structure that have high structural strength but have low mass transfer area. As the knowledge in mass transfer became more advance, it was soon discovered that the absorption process is actually a mass transfer process. One of the parameters that affect mass transfer is mass transfer area. The current generations of packing elements are made of flexible structure that provide high mass transfer area but have low structural strength. The current challenge is to develop the next generation of packing elements that have the qualities of both the previous and current generation.

The new packing element was made using a simple apparatus which is commonly found in domestic market which is baby bottle cleaner. 3 of the items were combined to form a single packing element. The packing element has rigid structures which provide strength and flexible structure which provide mass transfer area. The physical characteristics of the new packing element such as geometric surface area, void fraction, and equivalent spherical diameter were measured and calculated. These characteristics were then compared with other existing packing elements in the industry.

The performance of the new packing element was gauged based on pressure drop performance and mass transfer performance. Two methods were used to analyze the pressure drop and mass transfer performance; analytical and experimental method. The pressure drop performance was analyzed analytically using Ergun's equation. The mass transfer performance was analyzed analytically using correlations developed by

Mackowiak (2011), Schultes (2011), and Higbie (1935). For experimental method, an absorber system was constructed for the new packing element. The system uses air-water countercurrent flow system. The absorber column was constructed using plumbing materials.

The packing characteristics of mirv-1 such as geometric surface area, void fractions, and equivalent spherical diameter of packing particle shows that mirv-1 is comparable with other packing elements used in the industry. Performance analysis using the stated equation and correlation also indicates that the performance of the new packing element is comparable with other existing packing elements. Besides that, experiments conducted on mirv-1 shows that the pressure drops and mass transfer performance of mirv-1 is within the acceptable range applied in the industry. Based on these results, it can be concluded that mirv-1 has proven itself and worthy to be further develop to increase its performance.

ACKNOWLEDGEMENT

TABLE OF CONTENTS

LIST OF FIGURES

LIST OF TABLES

NOMENCLATURE

η_A = Mass transfer rate [mol/s]

k_C = Mass transfer coefficient [m/s]

A = Effective mass transfer area [m^2]

ΔC_A = Driving force concentration difference [mol/m^3]

β_L = Liquid-phase mass transfer coefficient [m/s]

a_e = Effective interfacial area for mass transfer per unit volume [m^2/m^3]

V = Volume occupied by packing [m^3]

a = Geometric surface area of packing per unit volume [m^2 /m^3]

h_L = Specific liquid hold-up [m^2/ m^3]

d_T = Mean droplet diameter [m]

u_L = Specific liquid load [m/s]

d_h = Hydraulic diameter [m]

l = Mean contact path [m]

φ_P = Form factor [-]

τ = Contact time [s]

$\Delta\rho$, $\rho_L - \rho_V$ = Differential density [kg/m^3]

σ_L = Surface tension of liquid [N/m]

ν_L = Kinematic viscosity [m^2/s]

Re_L = Reynolds Number [-]

g = Gravitational acceleration, 9.81 m^2/s

D_L = Diffusion coefficient of liquid [m^2/s]

Δp = Pressure drop across the packed bed (kg/m.s)

L = Length of the packed bed (m)

D_P = Equivalent spherical diameter of the packing (m)

ρ = Density of fluid (kg/m^3)

μ = Dynamic viscosity of the fluid (kg/m.s)

V_S = Superficial velocity of fluid (m/s)

ε = Void fraction

CHAPTER 1

INTRODUCTION

1.1 Background of Study

Packed towers are equipment that has packed bed installed in the internal of the equipment. Packed towers are widely used in industry to perform separation process such as absorption, stripping and distillation. Besides that, packed towers are also used as a reaction vessel for catalytic chemical reaction which involves solid catalyst contacting against fluid phase reactants. Below is the figure showing a typical packed tower absorber:
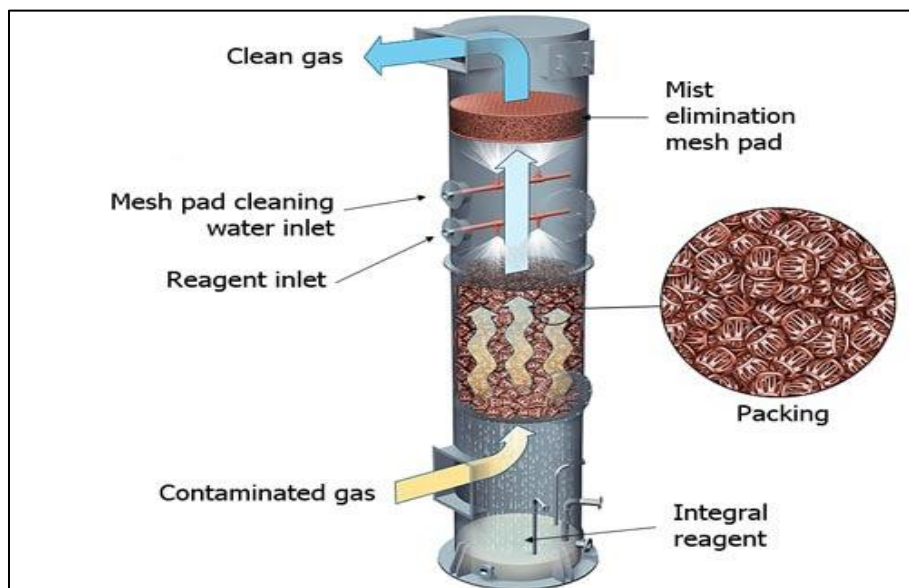
Figure 1: Packed bed absorber (Courtesy of ACTOM (Pty) Ltd)

For a typical packed bed absorber, the liquid solvent is introduced at the top of the packed bed in order for the solvent to wet the packing. A liquid distributor is used achieve even distribution of solvent across the packing. The gas is fed from the bottom of the column so that the gas will contact the solvent counter-currently to strip off any impurities in the gas.

1.2 Packing Elements

The packed bed is a fixed bed filled with packing elements. The function of the packed bed is typically to improve contact between two phases of fluid in process. The packed bed can be divided into types; Random packed bed, and Structured packed bed.

For random packed bed, the packed bed is randomly filled with small object like the Raschig ring (**Fig.2**). For structured packed bed, the packed bed is filled with structured section as shown in **Figure 3**.

Figure 2: Raschig ring

Figure 3: Structured packing

The development of modern random dumped packing for random packed bed, in the recent years, has made the random packed bed to have an established role the field of mass transfer processes. This is particularly due to the fact that random dumped packing display process properties approximately the same as the structured packing, and at the same time meet the advantages of the mass transfer trays.

The figure below shows the history of random dumped packing development since its introduction to the industry.
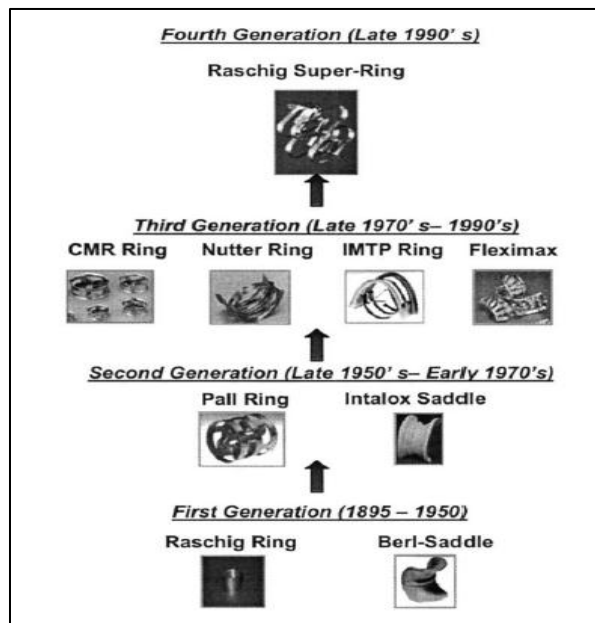
Figure 4: History of random dumped packing development

Based on Figure 4, the development of random dumped packing element has been done since its first introduction in the year 1895. The development of this packing element is shown by the evolving of the types and shapes of the packing element created by the leading companies in packing manufacturing.

The Raschig Super Ring plays an important role since it is known as the first random dumped packing of the fourth generation. Since its introduction to the market in 1995, numerous mass transfer columns have been packed with Raschig Super Rings in various chemical processes, petrochemical, refining, and environmental applications (Schultes. M., 2003).

1.3 Problem Statement

The development of packing element for packed columns has shown great progress since its first usage in the industries through Raschig Rings and Berl-Saddle. The structure of the first generation packing involves the usage of rigid structure. As understanding on packing element and mass transfer improved, the structure of packing evolves from a rigid structure to a flexible structure where large mass transfer area is available as compared to packing with rigid structure, as we can see in Raschig Super Rings.

The drawback of the new generation packing element is that, eventhough the packing can provide high mass transfer area, the flexible structure will get crushed or deformed at the bottom of a packed tower if the packing height is high. This is due to the weight of the top packing exerting force to the bottom packing.

The current challenge is to develop a next generation of packing element that will be able to address the drawback in the new generation of packing element. The next generation packing element can be a combination of the rigid structure of the previous generation packing elements and the flexible structure of the new generation of packing elements. The rigid structure is expected to provide support while the flexible structure will provide a large surface area for mass transfer.

4

Besides that, the next generation packing element is expected to be able compete against other industrially recognized random dumped and structured packing available in the market.

1.4 Objectives

The objectives of this project are:

- To develop a new type/design of packing element for packed towers.
- To study the characteristics/performance of the newly developed packing element and compare it against other existing packing elements present in the market.

1.5 Scope of Study

In order to accomplish these objectives, the project is divided into few phases to ensure that the project is completed systematically. The scope of study for the project is illustrated in the flow chart as follows:

Feasibility study of the project title
In this stage of the project, preliminary research work is done to identify the current packing elements available in the industry, set the purpose of study for this project, and identify feasible methods to accomplish the project.

Study on the characteristics/performance of the new packing element
In this stage of the project, the characteristics/ performance of the new packing element will be analyzed through experimentation and/or using developed mathematical model of random packed columns for gas-liquid system.

Development of new packing element

Depending on the time and resources available, a number of different types of packing elements will be developed and produced for experimentation.

Comparing the performance of the new packing element against existing packing elements in industry

In this stage of the project, the performance of the new packing element will be compared against existing packing elements in industry through existing data available for comparison.

Data interpretation

Final conclusion will be deduced based on the results from the study on the characteristics/performance of the new packing element and the comparison the performance of the new packing element against existing packing elements in the industry.

Documentation of the project/research

All works related to the project will be documented and submitted to the FYP committee.

Figure 5: Flow chart of the project

CHAPTER 2

LITERATURE REVIEW

2.1 Mass Transfer Efficiency

Based on the formula for mass transfer rate:

$$\eta_A = k_C.A.\Delta C_A \qquad [mol\,s^{-1}] \qquad (1)$$

In order to achieve highest mass transfer rate, all the 3 parameter on the right-hand side of the equation; mass transfer coefficient, k_C, effective mass transfer area, A, and driving force concentration difference, ΔC_A, must be maximized.

The driving force concentration difference, ΔC_A, is dependent on the process and is not affected by the packing in the packed tower. The only parameters that can be affected by the design of packing are mass transfer coefficient, k_C, and effective mass transfer area, A.

Model for prediction of liquid-phase mass transfer of random packed columns for gas –liquid system has been develop by Jerzy Mackowiak in 2011. The new equation for prediction of the volumetric mass transfer coefficient in the liquid phase, $\beta_L.a_e$, was derived on the basis of the assumption that liquid flows down in packed bed mainly in the form of droplets and that effective interfacial area for mass transfer per unit volume, a_e, depends on the hold up in packed bed.

The formula for volumetric mass transfer coefficient were developed based on the combination of equations developed for liquid-phase mass transfer coefficient, β_L, and effective interfacial area for mass transfer per unit volume, a_e.

$$\eta_A = k_C.A.\Delta C_A = \beta_L.a_e.V.\Delta C_A \qquad [mol\ s^{-1}] \qquad (2)$$

The Effective mass transfer area, A, in equation (1) is the same as the product of effective interfacial area for mass transfer per unit volume, a_e, and volume occupied by packing, V. According to Mackowiak (2011), the effective interfacial area for mass transfer per unit volume, a_e, is identical to the droplet surface, while the total liquid hold-up, h_L, corresponds to the liquid hold-up of the droplet. Therefore, it is possible to determine the effective interfacial area for mass transfer per unit volume, a_e, by using the following equation:

$$a_e = 6 \cdot \frac{h_L}{d_T} \qquad [m^2/m^3] \qquad (3)$$

According to equation (3), the effective interfacial area for mass transfer per unit volume, a_e, is directly proportional to the specific liquid hold-up, h_L, and is inversely proportional to the mean droplet diameter, d_T.

Formula for specific liquid hold-up is dependent on the flow regime across the packed bed. The flow regime, whether turbulent or laminar, can be determined through Reynolds Number, Re_L. The formula for Re_L is

$$Re_L = \frac{u_L}{a \cdot v_L} \qquad (4)$$

According to Mackowiak (2010), the specific liquid hold-up, h_L, in random packing for turbulent flow, $Re_L \geq 2$:

$$h_L = 0.57 \cdot \left(\frac{u_L^2 \cdot a}{g} \right)^{1/3} \qquad [m^2/m^3] \qquad (5)$$

For laminar flow, $0.16 < Re_L < 2$:

$$h_L = 0.75 \cdot \left(\frac{3}{g}\right)^{1/3} \cdot a^{2/3} \cdot (u_L \cdot v_L)^{1/3} \qquad [m^2/m^3] \qquad (6)$$

Based on equation (5) and (6), the effective interfacial area for mass transfer per unit volume, a_e, is directly proportional to the geometric surface area of packing per unit volume, a, which is determined by the design of the packing.

Therefore, packing design with high surface area per volume of packing will contribute to high effective interfacial area for mass transfer per unit volume, a_e.

Effective interfacial area for mass transfer per unit volume, a_e, is inversely proportional to the mean droplet diameter, d_T. The formula to determine mean droplet diameter, d_T, is as follows:

$$d_T = \sqrt{\frac{\sigma_L}{\Delta\rho \cdot g}} \qquad [m] \qquad (7)$$

Based on equation (7), the mean droplet diameter is directly proportional to the surface tension of the liquid, σ_L, and is inversely proportional to the density difference between liquid and gas, $\Delta\rho = \rho_L - \rho_V$. Therefore, the mean droplet diameter is not affected by the packing design.

According to Higbie (1935), the formula for determining liquid-phase mass transfer coefficient is as follows:

$$\beta_L = \frac{2}{\sqrt{\pi}} \sqrt{\frac{D_L}{\tau}} \qquad [m/s] \qquad (8)$$

Based on equation (8), the liquid-phase mass transfer coefficient is directly proportional to the diffusion coefficient in the liquid phase, D_L, and is inversely proportional to the contact time, τ. According to Schultes (2011), the contact time, τ, is

described as the time that a droplet needs to cover the distance, l, between two contact points within the packing.

$$\tau = \frac{l}{\bar{u}_L} \qquad [s] \qquad (9)$$

$$\bar{u}_L = \frac{u_L}{h_L} \qquad [m/s] \qquad (10)$$

By substituting equation (9) into (10), we obtain equation (11):

$$\tau = \frac{l \cdot h_L}{u_L} \qquad [s] \qquad (11)$$

For mean contact path, l, the following formula is used:

$$l = 0.115 \cdot \left(1 - \varphi_P\right)^{2/3} \cdot d_h^{1/2} \qquad [m] \qquad (12)$$

For hydraulic diameter, d_h, the following formula is used:

$$d_h = \frac{4 \cdot \varepsilon}{a} \qquad [m] \qquad (13)$$

The mean contact path, l, is dependent on the packing design. This is because the form factor of packing, φ_P, is dependent on the packing design. The table below shows some of the packing data for industrially recognized packing:

Table 1: Overview of technical data of packing used for calculating volumetric mass transfer coefficient, $\beta_L.a_e$

Packing	Symbol	$d \times 10^3$ (m)	ε (m³/m³)	a (m²/m³)	$N \times 10^3$ (1/m³)	d_S (m)	H (m)	$u_L \times 10^3$, from–to (m/s)	t_L (°C)	φ_P (–)
(a) Classic, non-perforated packing elements										
Raschig ring	◇	15	0.626	239.3	–	0.10	1.0	1.7–11	20–40	0
Ceramic	◆	50	0.782	100	6300	0.3	0.75	1–22.5	20	0
Intalox saddle ceramic	✧	38	0.757	125.7	18.9	0.3	1.4	1–11	21	0
(b) Packing elements with slightly perforated walls										
	◓	15	0.964	380	243.2	0.3	0.87	1–11	22.5	0.28
	○	25	0.954	223.5	53.9	0.3	1.46	1–11	21.5	0.28
Pall ring metal		s = 0.4								
	◔	25	0.942	232.1	55.6	0.15	1.3	0.79–10	22.5	0.28
	◍	35	0.946	150	19.6	0.3	1.4	1.2–8	19.5	0.28
	◑	38	0.952	149.6	15.8	0.3	1.46	1–11	20	0.28
	●	50	0.95	115.4	6.4	0.3	1.36	1–12	22.5	0.28
	□	25	0.894	238	55.18	0.3	1.4	1–10	23	0.309
Pall ring plastic (PP)	⊠	35	0.905	160	18	0.3	1.4	1–10	20	0.309
	■	50	0.93	111	6.85	1.0	1.65	1–18	20	0.309
	■	50	0.92	110	6.7	0.3	1.35	1–15	22	0.309
Pall ring ceramic	⊞	50	0.78	120	6.4	0.22	1	1–12	20	0.430
	▦	12	0.934	403	443	0.3	0.9	1–11	17.5	0.158

The volumetric mass transfer coefficient, $\beta_L.a_e$, is a product of equation (3) and (8). By substituting equation (5), (6), and (7) into equation (3), and equation (5), (6), (11), and (12) into equation (8), the following formula for volumetric mass transfer coefficient, $\beta_L.a_e$, can be obtained:

For turbulent liquid flow across packed bed, $Re_L \geq 2$:

$$\beta_L \cdot a_e = 15.07194 \cdot \left[\frac{\Delta\rho^{1/2} \cdot g^{1/3} \cdot D_L^{1/2}}{(1-\varphi_P)^{1/3} \cdot d_h^{1/4} \cdot \sigma_L^{1/2}} \right] \cdot u_L^{5/6} \cdot a^{1/6} \qquad [1/s] \qquad (14)$$

For laminar liquid flow across packed bed, $0.16 < Re_L < 2$:

$$\beta_L \cdot a_e = 20.7628 \cdot \left[\frac{\Delta\rho^{1/2} \cdot g^{2/3} \cdot D_L^{1/2} \cdot \nu_L^{1/6}}{(1-\varphi_P)^{1/3} \cdot d_h^{1/4} \cdot \sigma_L^{1/2}} \right] \cdot u_L^{2/3} \cdot a^{1/3} \qquad [1/s] \qquad (15)$$

Based on equation (14) and (15), the volumetric mass transfer coefficient, $\beta_L.a_e$, is proportional to the geometric surface area of the packing per unit volume, a. This shows that the volumetric mass transfer coefficient, $\beta_L.a_e$, is affected by the design of packing.

Besides that, equation (14) and (15) also shows that the volumetric mass transfer coefficient, $\beta_L.a_e$, is proportional to specific liquid load in relation to full column cross section u_L. Liquid load is defined as the ratio of the liquid mass flow to the gas mass flow.

If the liquid load is very low, the value for effective interfacial area for mass transfer per unit volume, a_e will also decrease eventhough the geometric surface area of packing, a, is large. This is because less liquid flow will cause less distribution of liquid across the bed, causing less mass transfer area.

2.2 Pressure Drop and Ergun's Equation

Pressure drop across a packed bed is one of the important performance parameters of a packing element. Low pressure drop during operation is desired because it will lead to low energy consumption for compressor to move gas across the packed column. Low energy consumption will lead to utility cost saving for operation of the packed column. One of the common equations used to predict pressure drop across packed bed is Ergun's equation.

The Ergun's equation was derived by the Turkish chemical engineer Sabri Ergun in 1952. By assuming $k_1=150$ and $k_2 = 1.75$, the equation expresses the friction factor, f_P, in a packed column as a function of the Reynold's number;

$$f_P = \frac{150}{Gr_P} + 1.75 \qquad [-] \qquad (16)$$

In the equation, f_P and Gr_P are defined as;

$$f_P = \frac{\Delta p}{L} \frac{D_P}{\rho V_s^2} \left(\frac{\varepsilon^3}{1-\varepsilon} \right) \qquad [-] \qquad (17)$$

$$Gr_P = \frac{D_P V_s \rho}{(1-\varepsilon)\mu} \qquad [-] \qquad (18)$$

Substituting equation (18) into (16), the following equation is obtained;

$$f_P = \frac{150(1-\varepsilon)\mu}{D_P V_s \rho} + 1.75 \qquad [-] \qquad (19)$$

Substituting equation (17) into (19), the following equation is obtained;

$$\frac{\Delta p}{L} \frac{D_P}{\rho V_s^2} \left(\frac{\varepsilon^3}{1-\varepsilon} \right) = \frac{150(1-\varepsilon)\mu}{D_P V_s \rho} + 1.75 \qquad [-] \qquad (20)$$

Solving for the pressure drop across packed bed, the following equation is obtained;

$$\Delta p = \frac{150(1-\varepsilon)^2 \mu V_s L}{D_P^2 \varepsilon^3} + \frac{1.75\rho V_s^2 L(1-\varepsilon)}{D_P \varepsilon^3} \qquad [kg/m.s] \qquad (21)$$

Based on equation (21), the pressure drop across a packed bed is inversely proportional to the void fraction of the bed, ε, and equivalent spherical diameter of the packing element. For a packing with high void fraction and large equivalent spherical diameter of the packing element, the pressure drop across the packed bed can be nearly zero.

Another important thing to be noted is that the pressure drop across a packed bed is directly proportional to the superficial velocity of fluid, density of fluid, and the length of packed bed in the column. Therefore, a column with long packed bed will have a higher pressure drop compared to column with shorter packed bed. Besides that, operation at high liquid and gas loading will cause high pressure drop across the packed bed.

This pressure drop equation is only applicable for gas flow only. The gas used for this project is air. The dynamic viscosity of air is 0.00001938 kg/m.s at 22.3 °C, which is the air temperature.

If k_1 and k_2 is not assumed, Ergun's equation will take the following form;

$$\frac{\Delta p}{L}\frac{D_P}{\rho V_s^2}\left(\frac{\varepsilon^3}{1-\varepsilon}\right)\left(\frac{D_P V_s \rho}{(1-\varepsilon)\mu}\right) = \left(\frac{D_P V_s \rho}{(1-\varepsilon)\mu}\right)k_2 + k_1 \qquad (22)$$

The constant k_2 describes the turbulence flow relation with the pressure drop across the packed bed, while k_1 describes the laminar flow relation with the pressure drop across the packed bed. This equation is a linear equation and value k_1 and k_2 can be compared between different packing elements. The common value for k_2 ranges between 1.5 and 1.8, while the common value for k_1 ranges between 150 and 180.

2.3 Packing Design for Packed Towers

Packing developers have continuously performed improvement on the packing line-up by developing new design of packing and conducting experiment for the newly designed packing.

Table 2: Packing particles

Packing Particle		Detail
Raschig ring	Berl-Saddle	• First generation packing particle for random dumped packed bed. • 1895 - 1950
Intalox Saddle	Pall Ring	• Second generation packing particle for random dumped packed bed. • 1950 - 1970
IMTP Ring	Nutter Ring	• Third generation packing particle for random dumped packed bed. • 1970 - 1990
Raschig Super Ring		• Fourth generation packing particle for random dumped packed bed. • 1995 - present

Based on the design of the packing particles, it can be observed that the structure of the packing particles have evolved from a rigid structure such as Raschig ring and Berl-Saddle, to a more open and flexible structure similar to Raschig Super Ring.

According to Dr. Subbarao, D. (2013), a combination of the rigid structure of the previous generation and the flexible structure of the new generation can be used to develop the next generation of packing element.

2.4 Wetted Wick

In 1989, Lee and Hwang conducted a series of experiments on a newly designed column called wetted wick column. Based on the column constructed by Lee and Hwang (1989), the inner surface of the wetted wick column is covered with a layer of capillary-porous materials and is wetted with a liquid phase solvent. The capillary porous materials are supported with wire clothes. Various porous materials such as cotton fiber glass and gauzes can be used as the wick. The figure below shows the schematic diagram of wetted wick absorption column:
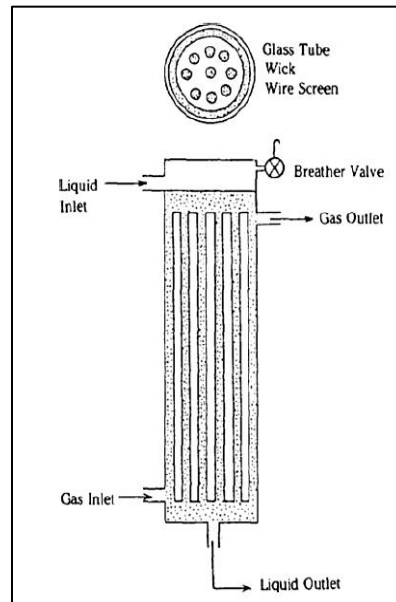
Figure 6: Schematic diagram of wetted-wick absorption column for higher efficiency

The construction of a packing using wick is a very ingenious idea. This is because, based on the construction material in which wicks are used to provide mass transfer area, this will create a very large geometric surface area available per volume of packing.

According to equation (11), (12), (13), and (14), the higher the geometric surface area of the packing, a, the higher the effective interfacial area for mass transfer per unit volume of packing, a_e.

According to Lee and Hwang (1989), the wetted-wick absorption column provides many features which improve the drawbacks that can be observed in conventional packed tower. The conventional packed towers have the following drawbacks that can cause conventional packed towers to be less appealing to industries:

- low liquid-gas interfacial area for mass transfer
- Non-uniform liquid distribution (channeling)
- Flooding
- Backmixing
- Excess wall flow of liquid

According to Lee and Hwang (1989), these drawbacks can be overcome by the wetted-wick absorption column as this new type of column features:

- Provides 100% wetted surface even at low liquid flowrate
- Does not create backmixing which can cause bad mass transfer
- Can be operated in the absence of gravity
- No wall flow of liquid
- Uniform distribution of liquid across the packing
- Fairly low pressure drop

CHAPTER 3

METHODOLOGY

This chapter will discuss on the methodology used for proceeding with the project.

| Designing the new type of packing element | → | Conducting experiment | → | Result and analysis |

3.1 Designing the New Type of Packing Elements

Next generation of packing element can be a combination of the rigid structure of the previous generation and a flexible structure of a new generation. The rigid structure is expected to provide strength while the extra fine flexible strands can increase the area. Search for the development of new packing element for packed bed absorber is in progress along the lines of the work of Lee and Hwang (1989) on wetted-wick columns.

3.2 Conducting Experiment

Once the new packing elements have been constructed, a series of experiments will be conducted to analyze the characteristics and performance of the newly developed packing element. Packing elements are evaluated primarily based on 2 aspects:

- Hydrodynamic performance
- Mass transfer efficiency

The hydrodynamic performance of the new packing element is evaluated based on the pressure drop of the packing element in a packed column. 2 methods will be applied to evaluate the pressure drop:

- Ergun's equation
- Pressure drop test using an air-water counter current flow (for both dry and wet packing)

The mass transfer efficiency of the new packing element is evaluated based on aspects such as mass transfer rate, HETP, volumetric mass transfer coefficient, and wetting efficiency. 2 methods will be applied to evaluate these aspects:

- Correlations by Mackowiak (2011), Schultes (2011), and Higbie (1935)
- Mass transfer experiment using an air-water counter current flow

Ergun's equation and correlations by Mackowiak (2011), Schultes (2011), and Higbie (1935) are used to evaluate the performance of the new packing against other packing element in the industry. This is because the other packing elements are difficult to obtained and tested with the current available facility.

3.2.1 Experiment Setup

Hydrodynamic test and mass transfer experiment were conducted using an air-water counter current flow experimental setup. The basic flow diagram for the experimental setup is shown in Figure 7. Figure 8 shows the dimension of the absorber column. Water and compressed air were used because these materials are available in the laboratory.
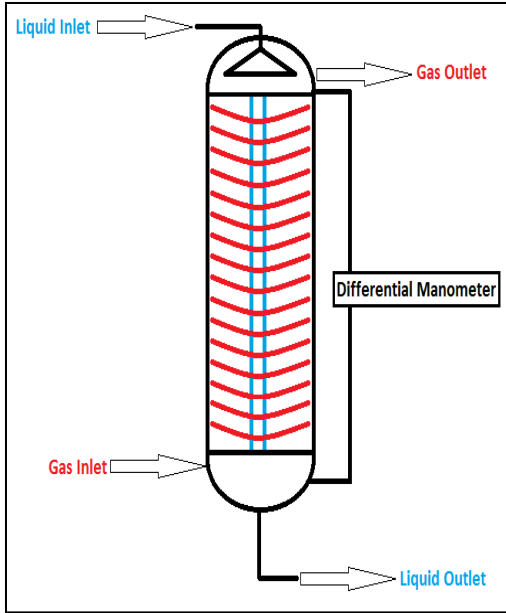
Figure 7: Basic flow diagram of the experimental setup
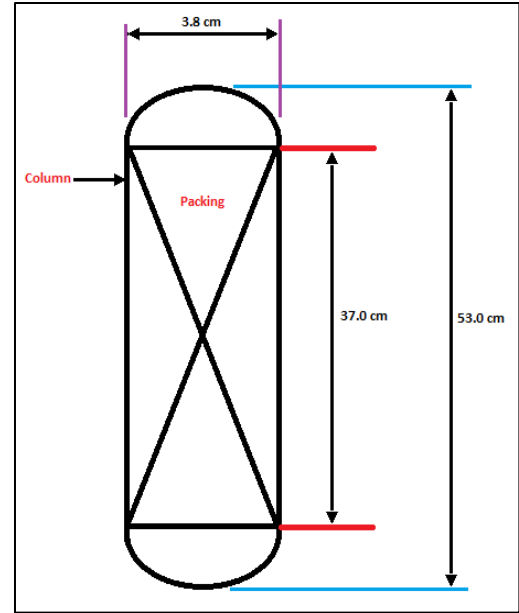
Figure 8: Column and packing dimension

Based on Figure 7, air is fed from the bottom side of the column and exited at the top side. Water is fed from the top side of the column and collected at the bottom side. The new packing element is placed in the middle of the column as shown in Figure 8. The new packing element will improve the contact between the two contacting medium.

The experimental setup is made up of plumbing materials which can be easily found in hardware shops. The column is made of PVC pipes. Holes are drilled in specific places to fit the manometer. The manometer is used to measure the pressure drop across the column. The manometer is made of flexible and transparent plastic tube. The manometer is filled with water as the medium to detect the pressure difference.

For the mass transfer experiment, the concept of air humidifier is used. By contacting air with water, some of the water will evaporate into the air causing the air humidity to increase. This phenomenon of humidifying the air can be considered as mass transfer phenomena. Therefore, the same aspect that increases the rate of mass transfer such as mass transfer area is applicable.

The humidity of inlet and outlet air is analyzed using dry-bulb and wet-bulb temperature. Four digital thermometers are used to measure the dry-bulb and wet-bulb temperature for both inlet and outlet gas flow. After obtaining the dry-bulb and wet-bulb temperature, psychometric chart is used to determine the amount of water in the air. By calculating the humidity difference between inlet and outlet gas flow rate, the amount of water evaporated to air can be determined. Multiplying the amount of water evaporated with mass flow rate of dry air, the rate of mass transfer can be obtained.

Figure 9: The experimental setup from different angle

Figure 10: The experimental setup

Figure 11: Gas outlet with digital thermometers

Figure 12: Gas inlet with digital thermometers

Figure 13: Column pressure drop manometer
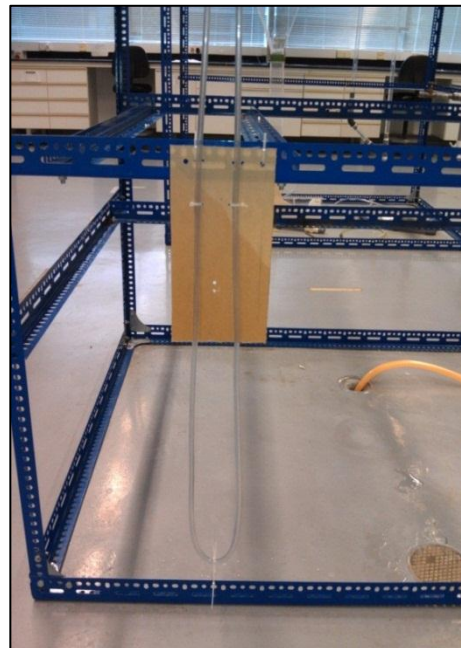
Figure 14: Orifice flow meter pressure difference manometer

3.2.2 Orifice Flow Meter Design
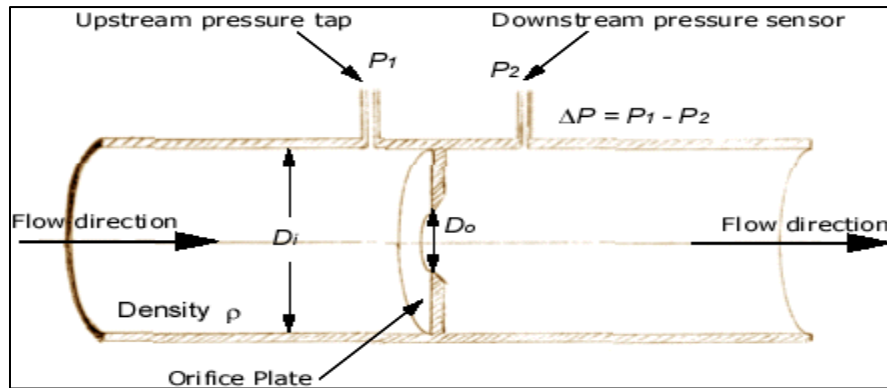
Figure 15: Basic flow diagram of orifice flow meter

In order to conduct the experiment, one of the parameters need to be measured is the inlet air flow rate through the absorber column. For the experiment, the fluid speed is assumed to operate below the subsonic region. For flow below the subsonic region, the incompressible Bernoulli's equation is applicable to describe the flow.

Applying the equation to a streamline travelling down the axis of the horizontal tube gives,

$$\Delta p = p_1 - p_2 = \frac{1}{2}\rho V_2^2 - \frac{1}{2}\rho V_1^2 \qquad [kg/m.s] \qquad (23)$$

Location 1 is positioned one orifice diameter upstream of the orifice, and location 2 is positioned one-half orifice diameter downstream of the orifice. From the continuity equation, the velocities can be replaced by cross-sectional areas of the flow and the volumetric flow rate, Q;

$$\Delta p = \frac{1}{2}\rho Q^2 \frac{1}{A_2^2}\left[1 - \left(\frac{A_2}{A_1}\right)^2\right] \qquad [kg/m.s] \qquad (24)$$

Solving for the volumetric flow rate Q gives;

$$Q = \sqrt{\frac{2\Delta p}{\rho}} \frac{A_2}{\sqrt{1-\left(\frac{A_2}{A_1}\right)^2}} \qquad \left[m^3/s\right] \qquad (25)$$

The above equation is only applicable to perfectly laminar and inviscid flows. For real flows, viscosity and turbulence are present and act to convert kinetic flow energy into heat. To account for this effect, a discharge coefficient, C_d is introduced into the above equation to marginally reduce the flowrate Q;

$$Q = C_d \sqrt{\frac{2\Delta p}{\rho}} \frac{A_2}{\sqrt{1-\left(\frac{A_2}{A_1}\right)^2}} \qquad \left[m^3/s\right] \qquad (26)$$

The actual flow profile at location 2 downstream of the orifice is complex, causing the effective value of A_2 uncertain. To make the calculation easier, the following substitution is made;

$$C_f A_O = C_D \frac{A_2}{\sqrt{1-\left(\frac{A_2}{A_1}\right)^2}} \qquad \left[m^2\right] \qquad (27)$$

A_O is the area of the orifice. As a result, the volumetric flow rate Q for real flows is given by the equation;

$$Q = C_f A_O \sqrt{\frac{2\Delta p}{\rho}} \qquad \left[m^3/s\right] \qquad (28)$$

The mass flow rate can be calculated by multiplying the volumetric flow rate with fluid density;

$$Q_{mass} = \rho Q \qquad \left[kg/s\right] \qquad (29)$$

For the experiment, the gas used is air. The pressure difference for the orifice is measured based on the difference in water height using a simple manometer made of transparent tube filled with water. The following equation is used to calculate the pressure difference;

$$\Delta p = \rho g h \qquad \left[kg / m \cdot s^2 \right] \qquad (30)$$

For the experiment, I have designed an orifice flow meter in order to measure the air flow rate entering the packed column. The basis of design for the designed orifice flow meter is summarized in the table below;

Table 3: Basis of design for the orifice flow meter

Pipe (inlet) diameter upstream of orifice D_i, cm	3.8
Pipe area upstream of orifice A_i, m^2	0.001134
Orifice diameter D_O, cm	1.3
Orifice area A_O, m^2	0.0001327
Water density, kg/m^3	1000
Gravitational constant, m/s^2	9.81
Flow coefficient, C_f	0.7

For the calculation of volumetric flow rate using equation (21), the density of air can be found in the psychometric chart based on the dry-bulb and wet-bulb temperature of the inlet air.

Based on the basis of design for the orifice, an Excel spreadsheet was made incorporating all this data and equations to calculate the air flow rate through the absorber column based on the pressure drop across the orifice.

3.2.3 Experiment Procedure

3.2.3.1 Dry Pressure Drop Experiment

1. Close the water outlet valve.
2. Open the air inlet valve until the water height in the orifice flow meter difference pressure manometer increase by 0.2cm.
3. Measure and record the water height increment in the column pressure drop manometer.
4. Repeat step 2 and 3 with water height of 0.4cm, 0.6cm, 0.8cm, 1.0cm, 1.3cm, 1.7cm, 2.5cm, 3.0cm, 3.5cm, 4.0cm in the orifice flow meter pressure difference manometer.

3.2.3.2 Mass Transfer Experiment

1. Open the water outlet valve until it is fully open.
2. Open the water inlet valve full for 15 minutes to make sure the packing element is fully wetted.
3. Close the water inlet valve partially to decrease the water flow rate.
4. Collect the amount of water flow in 10 seconds using measuring cylinder and record the value.
5. Close the water outlet valve partially to prevent air escaping through the water outlet valve.
6. Attach wet tissue papers to one of the 2 digital thermometers probes at the inlet and outlet of gas flow.
7. Open the gas inlet valve partially until the water height in the orifice flow meter pressure difference manometer increase by 0.4cm.
8. Let the equipment run for 5 minutes.
9. Record the wet-bulb and dry-bulb temperature of both inlet and outlet gas flow.
10. Record the water height increment in the column pressure drop manometer.

11. Repeat step 7 to 10 with water height of 0.8cm, 1.0cm, 1.2cm, 1.4cm, 1.8cm, and 2.3cm.

3.3 Result and Analysis

Once the results have been recorded, the results will be analyzed and compared with performance of packing from other literatures. The performance parameters analyzed includes:

- Geometric surface area of packing, a.
- Void fraction of packing, ε.
- Pressure drop per meter of packing length.
- Mass transfer rate
- Wetting efficiency
- Volumetric mass transfer coefficient

3.4 Tools Required

The following tools and raw materials may be required to accomplish the project:

Table 4: Tools and raw materials required

Hardware	Raw materials	Software
Handsaw Table drill Knife Digital thermometers	Air Water Baby bottle's cleaner PVC cement PVC Pipe PVC fittings PTFE tape Duct tape Plastic hose Insulators	Microsoft Word - for documenting the findings and results of the project. Microsoft Excel - used for calculation, making datasheet and graphs for analysis.

Table 5: Gantt chart

Activities	FYP 1														FYP 2													
	1	2	3	4	5	6	7	8	9	10	11	12	13	14	1	2	3	4	5	6	7	8	9	10	11	12	13	14
Selection of topic	▓	▓																										
Critical literature review on packing design, model for mass transfer efficiency, pressure drop across bed, and experimental set-up		▓	▓	▓	▓	▓	▓	▓	▓																			
Submission of Extended Proposal						▓																						
Producing packing prototype							▓	▓	▓		▓	▓	▓	▓														
Submission of Interim Draft Report													▓															
Submission of Interim Report														▓														
Experimental work on evaluation of mass transfer performance of the new packing element.																▓	▓	▓	▓	▓	▓	▓	▓					

Activities	FYP 1														FYP 2													
	1	2	3	4	5	6	7	8	9	10	11	12	13	14	1	2	3	4	5	6	7	8	9	10	11	12	13	14
Data analysis and interpretation															■	■	■	■	■	■	■	■	■					
Result validation based on literature data																				■	■	■	■	■	■	■		
Documentation of research work		■	■	■	■	■	■	■	■	■	■	■	■	■	■	■	■	■	■	■	■	■	■	■	■	■	■	■

CHAPTER 4

RESULTS AND DISCUSSION

4.1 Developing the New Packing Element

As described in the earlier sections, the next generation of packing element will be a combination of the rigid structure of the previous generation and the flexible structure of the new generation.

For the first prototype, a common item in our daily life is used to make the packing element, which is a baby's bottle cleaner. 3 of this item were connected together using wires as shown in Figure 16 and Figure 17.
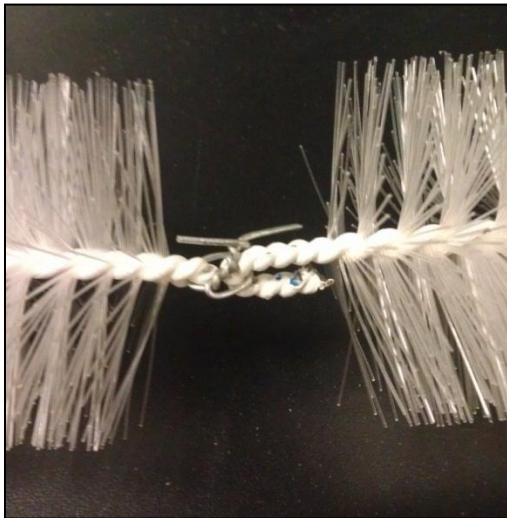

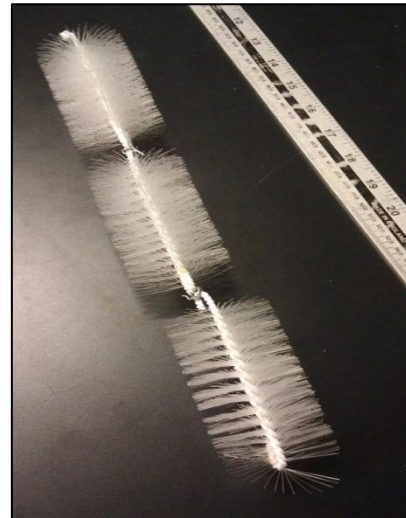**Figure 16**: Connection between packing sections

Figure 17 : The new packing at a glance

It can be observed that this packing element now has combination of rigid structure and flexible structure. The white-colored rod represents the rigid structure which provides strength and support while the thin transparent fibers represent the flexible structure which provides high mass transfer area.

This first prototype of the next generation packing element is named **mirv-1**.The new packing element's length was measured using a ruler. The length of the new packing element was approximately 37.0 cm.
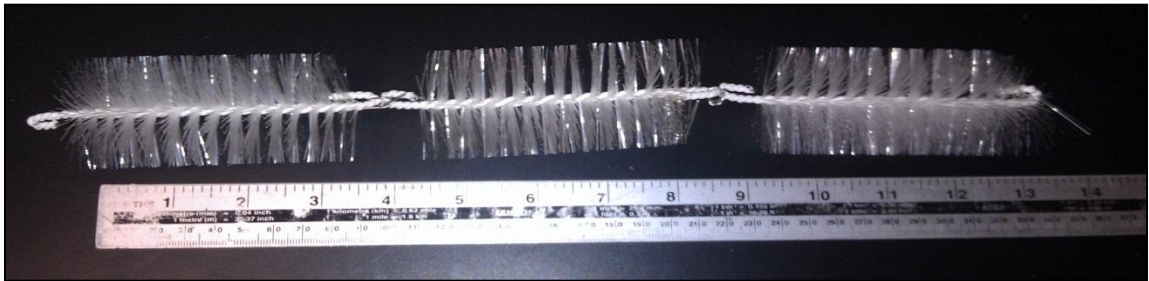

Figure 18: Packing length being measured

4.2 Finding the Geometric Surface Area and Volume of the New Packing Element

The volume of the packing is an important parameter to be determined because the void fraction of the packing in the absorber column can only be determined if the volume of the packing is known. Two methods were used to determine the volume of the packing:

- Water Displacement Method
- Manual Calculation Method

4.2.1 Water Displacement Method

A 100.0ml beaker was placed in a transparent plastic container. The beaker was then filled with water until some of the water spilled from the beaker due to fully filled. The spilled water in the plastic container was then wiped away with tissue.

After that, the packing element was then immersed into the beaker filled with water until the packing element is fully submerged as shown in Figure 19. The volume of spilled water collected was then measured using a measuring cylinder as shown in Figure 20.
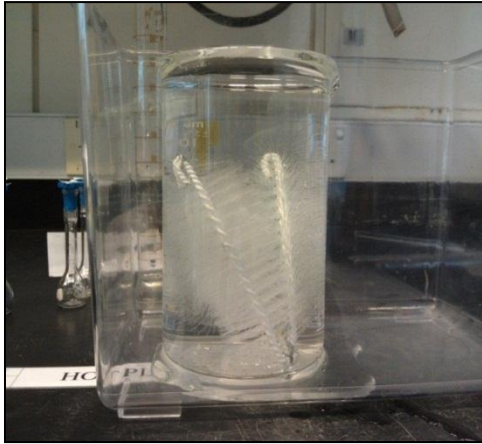

Figure 19: Measuring packing element volume using water displacement method

Figure 20: Volume of water displaced for the packing element

This procedure was applied 3 times for the packing element. Table 5 shows the volume of the packing obtained after 3 trials.

Table 6: Packing volume obtained using water displacement method

Trial	Packing Volume (mL)
1	25.0
2	21.0
3	20.0

Based on the 3 trials made, the average volume of the packing is

$$Volume\ of\ the\ packing\ at\ height,\ H = \frac{25.0\,mL + 21.0\,mL + 20.0\,mL}{3} = 22.0\,mL$$

$$= 22.0\,mL \times \frac{1.0\,L}{1000.0\,mL} \times \frac{1.0\,m^3}{1000.0\,L} = 2.2 \times 10^{-5}\,m^3$$

The height of the packing in the column, H, is 37.0 cm. Therefore, the packing surface area will be:

$$Geometric\ Surface\ Area\ of\ the\ Packing = \frac{2.2 \times 10^{-5}\,m^3}{\left(37.0\,cm \times \dfrac{1.0\,m}{100.0\,cm}\right)} = 5.9459 \times 10^{-5}\,m^2$$

4.2.2 Manual Calculation

The manual calculation method uses some simple principles in determining the volume of the packing. The method is explained briefly in the next paragraph.

First, the thickness and length of the flexible and rigid structure are determined by using a micrometer:

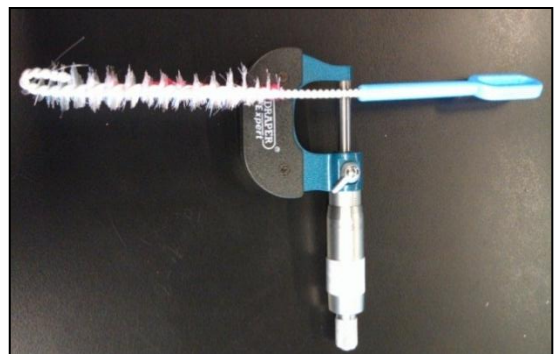**Figure 21**: Measuring flexible structure diameter

Figure 22: Measuring rigid structure diameter

Based on the measurement obtained from the micrometer, the diameter and volume for the flexible and rigid structure are calculated as follows:

Diameter of the flexible structure $= 0.305$ mm $= 3.05$ x 10^{-4} m
Length of the flexible structure $= 2.3$ cm $= 2.3$ x 10^{-2} m
Surface area of a flexible structure $= (3.142)*(3.05$ x 10^{-4} m)*(2.3 x 10^{-2} m)
$= 2.2114$ x 10^{-5} m^2

Volume of a flexible structure $= (3.142)*(3.05$ x 10^{-4} m)^2 *(2.3 x 10^{-2} m)*(0.25)
$= 1.6806$ x 10^{-9} m^3

Diameter of the rigid structure $= 3.61$ x 10^{-3} m
Length of the rigid structure $= 42.1$ x 10^{-2} m
Surface area of the rigid structure $= (3.142)*(3.61$ x 10^{-3} m)*(42.1 x 10^{-2} m)
$= 4.7957$ x 10^{-3} m^2

Volume of the rigid structure $= (3.142)*(3.61$ x 10^{-3} m)^2 *(42.1 x 10^{-2} m)*(0.25)
$= 4.3097$x 10^{-6} m^3

Second, the numbers of flexible structure per stick of the baby's bottle cleaner are determined. A same baby's bottle cleaner was used. All the flexible structures were cut off from its rigid structure and collected.

Figure 23: The flexible structures of the new packing element

After that, 10 of the longest strands were selected from the pile of flexible structures and weighted using a digital balance. The following were the results obtained:

Weight of paper   = 1.6780 g
Weight of 10 pieces of flexible structures = 1.7107 g
Weight of a piece of flexible structure = (1.7107 g – 1.6780 g)/10 = 0.00327 g

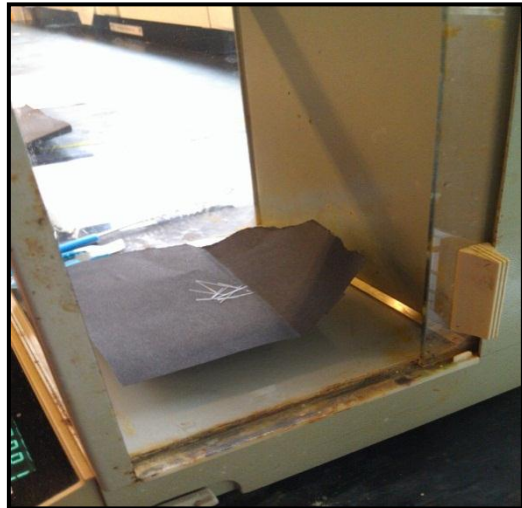**Figure 24:**10 flexible structures   **Figure 25**: Weighing 10 flexible structures

After that, the total weight of the flexible structures is measured. The following are the results:

Weight of beaker   = 107.1787 g
Weight beaker + flexible structures = 111.6140 g
Weight of flexible structures   = 111.6140 g - 107.1787 g = 4.4353 g

Figure 26: All the flexible structures   **Figure 27**: Weighing all the flexible structures
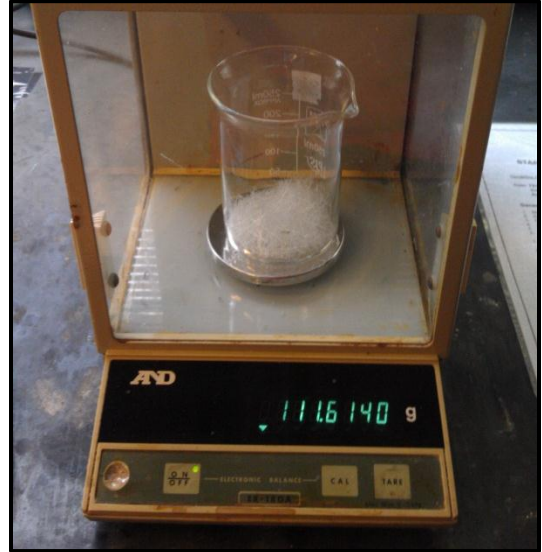
Therefore, the number of flexible structure per stick is

(4.4353 g)*(1.0 piece / 0.00327 g) = 1356.36 pieces

Figure 28: The rigid structure

Taking into account the leftovers on the rigid structure, the approximate number of flexible structure is approximately 1450 pieces per stick of baby's bottle cleaner.

Based on this number, the geometric surface area and volume of the packing are able to be calculated. The newly developed packing is made of 3 baby's bottle cleaner. By assuming that all the 3 items are identical and have the same number of flexible structures, the following parameters are calculated:

Geometric surface area of the packing $= 0.10099 \text{ m}^2$
Volume of the packing at height H $= 1.162 \times 10^{-5} \text{ m}^3$

The comparison of results obtained through the water displacement method and manual calculation method is shown in Table 7.

Table 7: Geometric surface area and volume of the packing based on water displacement method and manual calculation method

Characteristics	Water Displacement Method	Manual Calculation Method
Geometric surface area of the packing, m^2	5.9459×10^{-5}	0.10099
Volume of the packing at height H, m^3	2.2×10^{-5}	1.162×10^{-5}

Based on the data obtained in Table 6, the data from manual calculation method will be used as the basis of design for the new packing element. This method is chosen because it gives a reasonable value for both geometric surface area of packing and volume of packing at height of 0.37m.

Besides that, the water displacement method was suspected to give value with some errors. The errors are:

- Air bubble formed along the flexible structures when the packing is submerged into the beaker filled with water.
- The displaced water cannot be fully collected because some of the water stick to the surface of the larger container.
- Parallax error is also possible because the volume is measured using measuring cylinder.
- Sensitivity of the measuring cylinder is low.

4.3 Determining the Packing Characteristics

The new packing element will be placed inside an absorber column made of PVC pipe. Figure 20 shows the approximate dimensions of the absorber column.

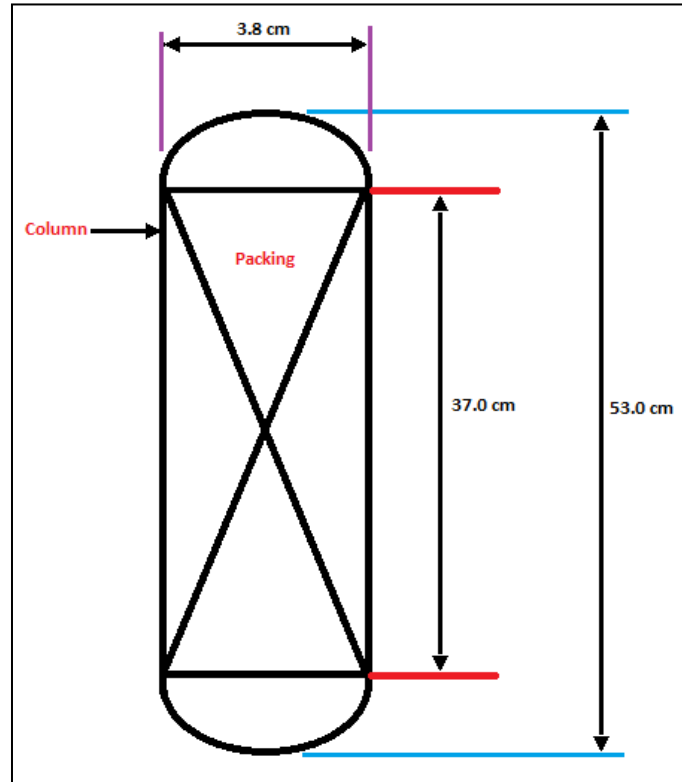**Figure 29**: Dimensions for the absorber column

The height of the packing in the column, H, is 37.0 cm. The volume of the column at height H is:

$$Volume\ of\ the\ column\ at\ height, H = \pi r^2 H = \frac{3.142}{4} \times (0.038\,m)^2 \times 0.37\,m = 4.196769 \times 10^{-4}\,m^3$$

Therefore, the geometric surface area of the new packing element per unit volume, a, is:

$$Geometric\ Surface\ Area\ of\ Packing\ per\ unit\ Volume, a = \frac{0.10099\,m^2}{4.196769 \times 10^{-4}\,m^3} = 240.6375\,m^2/m^3$$

The void fraction, ε, of the new packing element inside the column is:

$$Void\ fraction, \varepsilon = \frac{Free\ Volume\ Available}{Total\ column\ volume} = \frac{(4.196769 \times 10^{-4}\,m^3) - (1.162 \times 10^{-5}\,m^3)}{4.196769 \times 10^{-4}\,m^3} = 0.972$$

The packing is made of plastic and is assumed to be slightly perforated. Therefore, the form factor, φ_P, is assumed to be similar to Pall Ring Plastic 35.0 mm, which is 0.309.

The characteristics of the new packing element are compared with other packing elements available in the market as shown in Table 8.

Table 8: Comparison between packing elements

Characteristics	mirv-1	Bialecki Ring Metal 12mm	VSP Ring Metal 50mm	Pall Ring Metal 25mm	Pall Ring Plastic 35mm
Geometric surface area per unit volume (m²/m³)	240.6375	403.00	95.30	232.100	160.000
Form Factor, φ_P	0.309	0.158	0.380	0.280	0.309
Void fraction, ε	0.972	0.934	0.982	0.942	0.905
Number of packing per unit volume (1/m³)	-	443000.00	7150.00	55600.00	18000.00
Equivalent spherical diameter of packing, D_P (m)	0.001475	0.017	0.065	0.036	0.053

Based on the results from Table 8, it can be concluded that the geometric surface area of packing per unit volume, a, for mirv-1 is exceptionally large and is comparable with other packing elements such as VSP Ring Metal 50mm, Pall Ring Plastic 35mm, and Pall Ring Plastic 25mm

Besides that, the void fraction, ε, for mirv-1 is high, highlighting a very low resistance to gas and liquid flow inside the column. This can cause the pressure drop inside the absorber column to be very low during operation.

4.4 Hydrodynamic Test: Pressure Drop

Hydrodynamic test at dry condition was successfully conducted for mirv-1. The experimental values are compared with calculated values obtained from equation (22). The Ergun's constants are assumed to be $k_1 = 150$ and $k_2 = 1.75$. Figure 30 shows the result obtained from the hydrodynamic test.

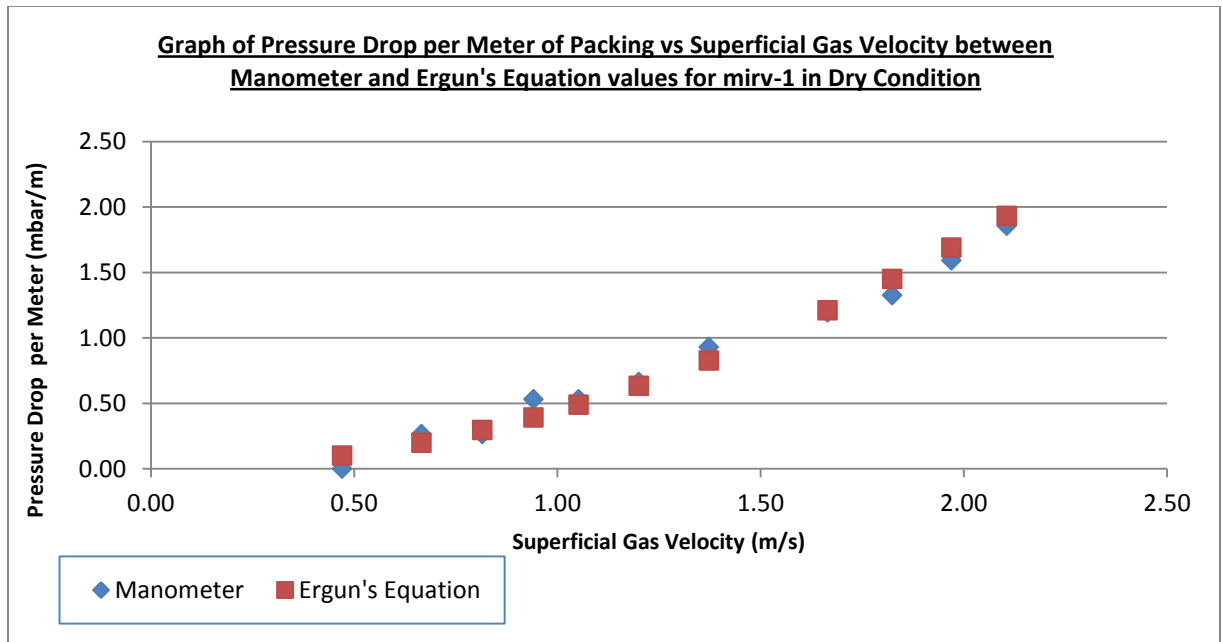**Figure 30**: Graph of Pressure Drop per Meter of Packing against Superficial Gas Velocity between Manometer and Ergun's Equation values for mirv-1 in Dry Condition

Based on Figure 30, the calculated values using Ergun's equation are almost similar with the experimented values with error less than 10.0% at most of the points. This shows that pressure drop of mirv-1 is describable using Ergun's equation.

Besides that, equation (22) is a linear equation and the assumed Ergun's constant k_2 can be compared with experimental value obtained from the hydrodynamic test.

$$\frac{\Delta p}{L}\frac{D_P}{\rho V_s^2}\left(\frac{\varepsilon^3}{1-\varepsilon}\right)\left(\frac{D_P V_s \rho}{(1-\varepsilon)\mu}\right)=\left(\frac{D_P V_s \rho}{(1-\varepsilon)\mu}\right)k_2+k_1 \qquad (22)$$

The value for the Y-axis is calculated using the left-hand side correlation which is:

$$\frac{\Delta p}{L}\frac{D_P}{\rho V_s^2}\left(\frac{\varepsilon^3}{1-\varepsilon}\right)\left(\frac{D_P V_s \rho}{(1-\varepsilon)\mu}\right)$$

The value for the X-axis is calculated using the right-hand side correlation which is:

$$\left(\frac{D_P V_s \rho}{(1-\varepsilon)\mu}\right)$$

The constant k_1 in the equation (22) is assumed to be 150. Based on equation (22) and packing characteristics of mirv-1 from Table 8, the value for X-axis and Y-axis are calculated at different superficial gas velocity. Figure 31 shows the plotted graph.
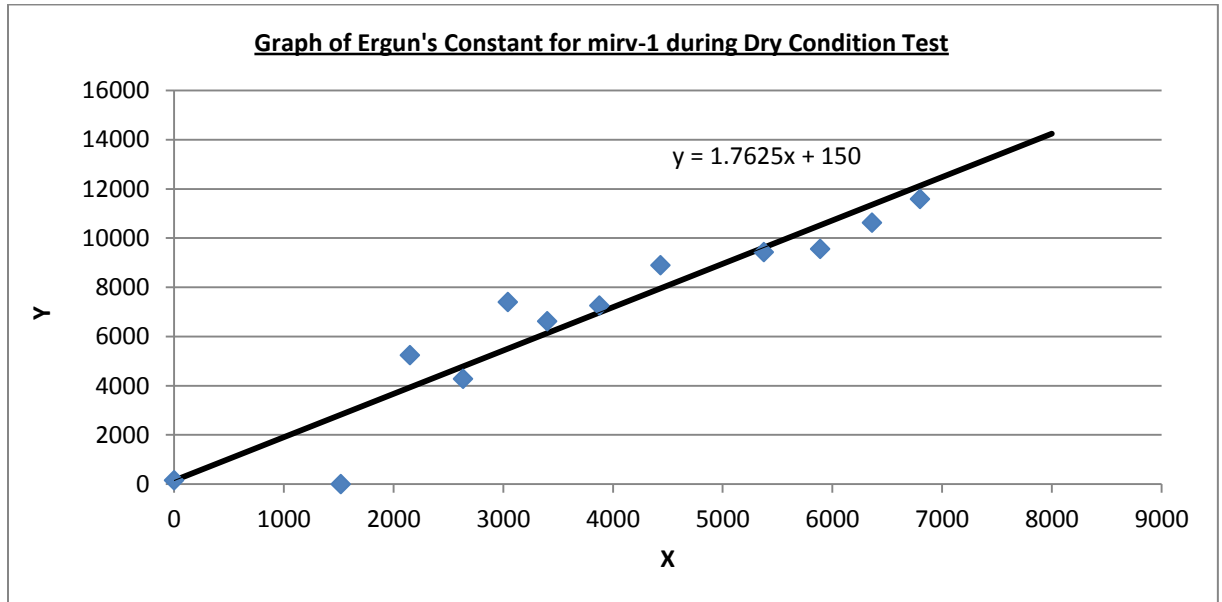

Figure 31: Graph of Ergun's Constant for mirv-1 during Dry Condition Test

40

Based on the trend line obtained in Figure 31, the experimental value for the Ergun's constant k_2 is 1.7625, which is 0.7% higher than the assumed k_2 value of 1.75. Therefore, the assumed value for Ergun's constant k_1 and k_2 can be used in equation (21) to compare the pressure drop of mirv-1 and other packing elements available in the industry.

It is difficult to obtain packing elements such as VSP Ring Metal 50mm, Pall Ring Plastic 35mm, Pall Ring Metal 25mm, and Bialecki Ring Metal 12mm. However, the characteristics of these packing elements such as void fraction and equivalent spherical diameter of packing are available as shown in Table 8. These data can be used in equation (21) together with the assumed value for the constants k_1 and k_2 to calculate the pressure drop of the packing elements at different superficial gas velocity. The calculated pressure drops of different packing elements are compared with the pressure drop of mirv-1 as shown in Figure 32.
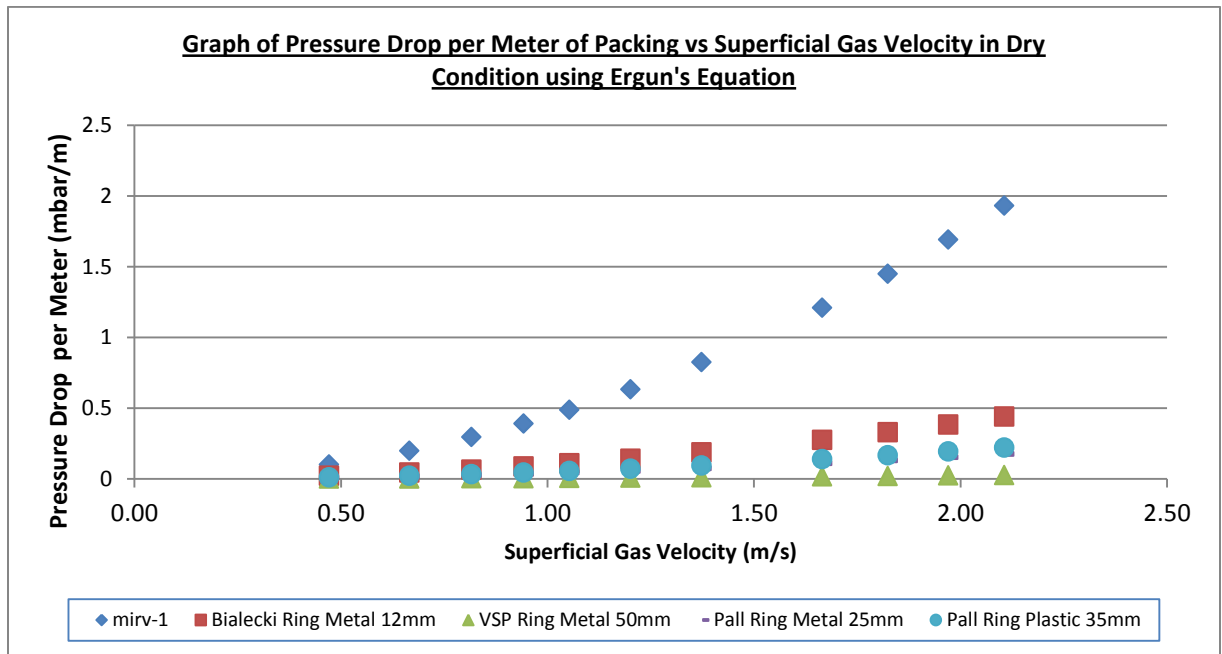

Figure 32: Graph of Pressure Drop per Meter of Packing vs Superficial Gas Velocity in Dry Condition using Ergun's Equation

Based on Figure 32, the pressure drop per meter of packing element for mirv-1 increases exponentially as the superficial gas velocity increases. At highest tested

superficial velocity of 2.11 m/s, the pressure drop of mirv-1 is 1.93mbar/m. Bialecki Ring Metal 12mm has the highest pressure drop per meter of packing element among the four packing elements available in industry. The value calculated for mirv-1 is approximately 3.4 times higher than the pressure drop per meter of packing element of Bialecki Ring Metal 12mm at the same superficial gas velocity.

The high pressure drop of mirv-1 compared to other packing elements is due to small equivalent spherical diameter of mirv-1. The pressure drop across packed bed is inversely proportional to equivalent spherical diameter of packing element as shown in equation (21). The equivalent spherical diameter of mirv-1 is approximately 11 times smaller than Bialecki Ring Metal 12mm, which has the smallest equivalent spherical diameter among the four packing elements available in industry.

However, the acceptable pressure drop in packed bed for absorber and stripper application ranges between 1.57mbar/m to 4.51mbar/m [11]. Even though the pressure drop performance of mirv-1 is inferior compared to other packing elements available in the industry, it is still in the acceptable range of pressure drop in packed bed for absorber application.

Besides dry condition test, pressure drop test with varying specific liquid load was also conducted for mirv-1. The test was conducted to study the effect of specific liquid load on pressure drop across packed bed. Figure 33 shows the result obtained from the test.
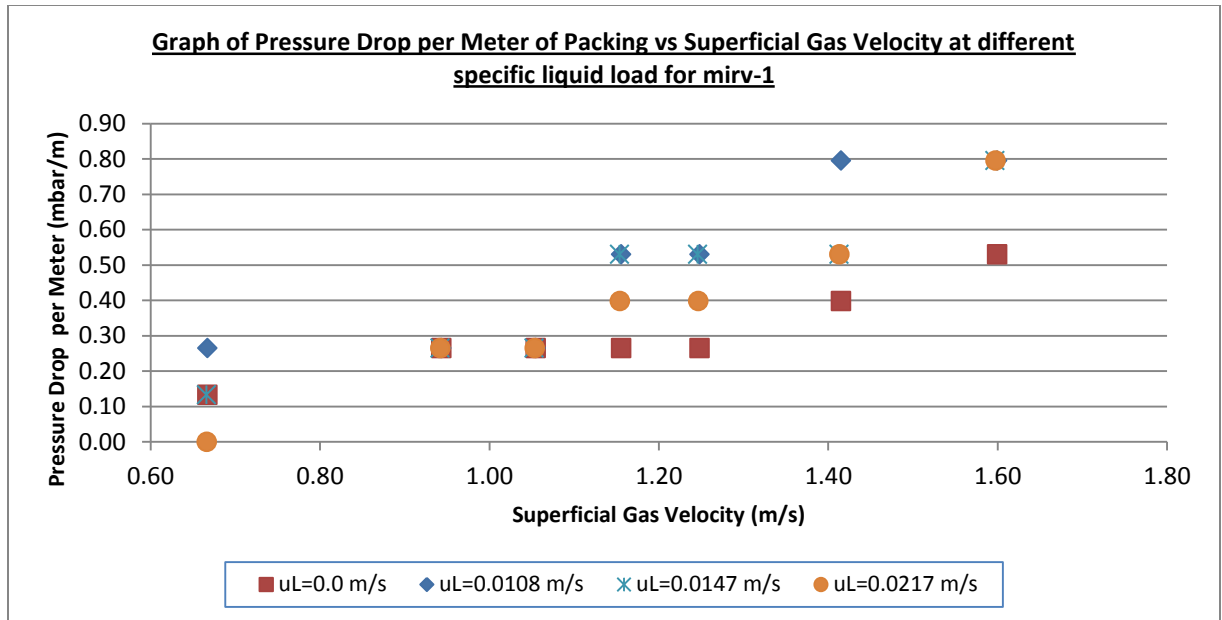
Figure 33: Graph of Pressure Drop per Meter of Packing vs Superficial Gas Velocity at different specific liquid load for mirv-1

Based on Figure 33, the pressure drop increases as the superficial gas velocity increases. This experimental result is same as the expected result. However, the pressure drop relation with specific liquid load is inconsistent. The expected result was that the pressure drop increases as the specific liquid load increases. This is because higher specific liquid load will induce more resistance towards upward air flow in the column. This resistance will contribute to increase in pressure drop across the packed bed.

The inconsistency found in the result is suspected due to the manometer used to measure the pressure drop across the packed bed. The manometer used is transparent rubber tube filled water, making the sensitivity of the manometer to be low. Besides that, the manometer can be considered to be poorly constructed. During the test run, some bubbles formed and got stuck inside the manometer, making the pressure drop reading to be inaccurate.

4.5 Mass Transfer Efficiency

4.5.1 Correlations by Mackowiak (2011), Schultes (2011), and Higbie (1935)

The performance of the new packing element, mirv-1, was evaluated using mathematical models and correlations developed by Mackowiak (2011), Schultes (2011), and Higbie (1935), which are equation (3), (4), (5), (6), (7), (8), (9), (10), (11), (12), (13), (14) and (15).

In order to use these mathematical models and correlations to evaluate mirv-1, an absorption system needs to be selected. The selected system will provide the necessary constants required to evaluate the performance parameters of mirv-1 as a function of specific liquid load, u_L.

Based on the work of Mackowiak (2011), the absorption system selected is as follows:

- System: CO_2 - water/Air
- System Pressure: 1.0 bar
- Liquid Temperature: 295.5 K
- Gas Capacity Factor, F_V : 0.96 $kg^{1/2}/m^{1/2}.s$

At this temperature and pressure, the constants for the system are found to be as shown in Table 9.

Table 9: Constants for CO_2 – water/ Air System

Gravity Acceleration (m/s^2)	9.810
Surface Tension of Water (kg /s^2)	0.07275
Kinematic Viscosity of Water(m^2/s)	0.000000961
Diffusion Coefficient (m^2/s)	0.0000000016

There is still one missing constants for the system which is the differential density, $\Delta\rho$. This constant depends on the concentration of CO_2 in the air during the experiment is conducted. The experimental result is available in the work of Mackowiak (2011). By using this experimental result, it is possible to use equation (14) and (15) to determine the differential density, $\Delta\rho$, during the experiment.

Figure 34 shows one of the experimental results based on the selected system. A packing element was selected as the basis in order to calculate the differential density, $\Delta\rho$. The packing element selected is:

- Packing: Pall Ring Metal 25.0mm
- Geometric Surface Area, a (m^2/m^3) = 232.1
- Form Factor, φ_P = 0.28
- Void Fraction, ε = 0.942

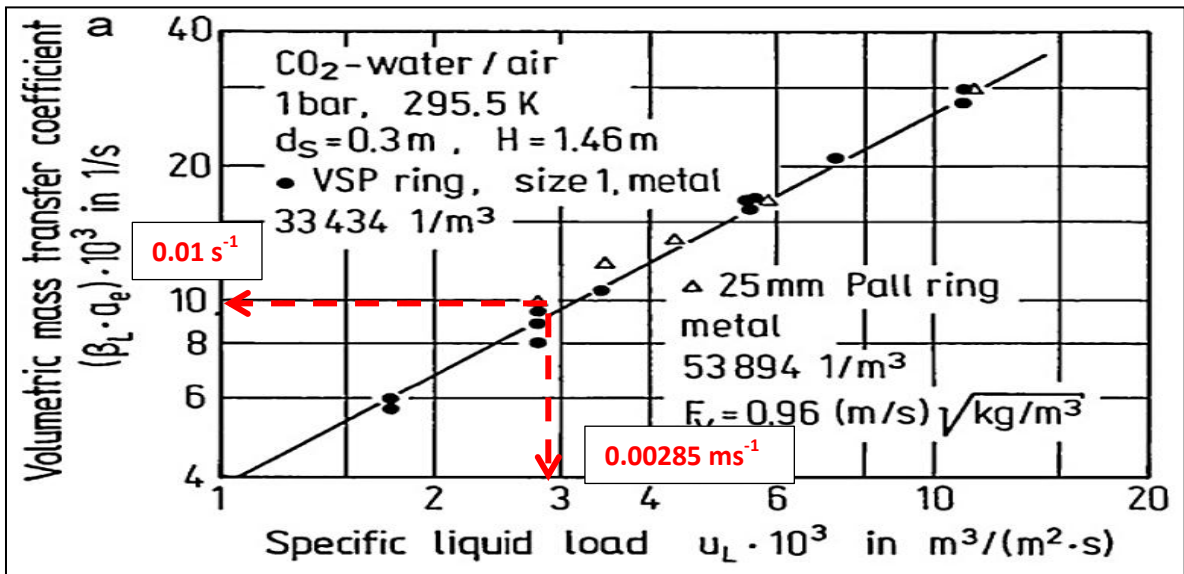**Figure 34**: Experimental data for volumetric mass transfer coefficient, $\beta_L.a_e$, as a function of Specific Liquid Load, U_L
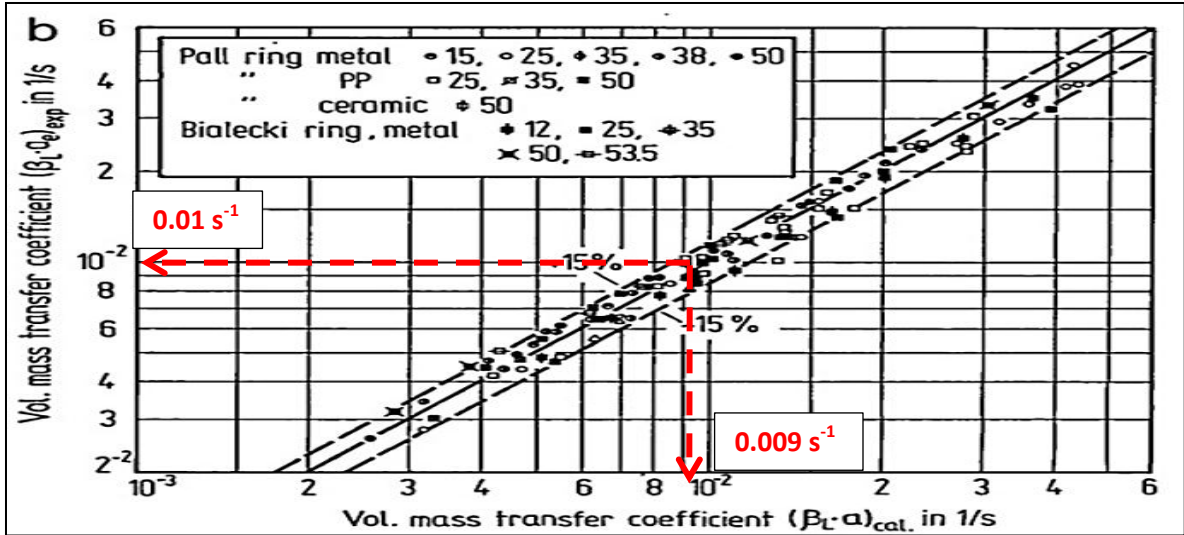
Figure 35: Comparison between experimental data and calculated data for volumetric mass transfer coefficient, $\beta_L.a_e$

Based on Figure 34, an experimental value for volumetric mass transfer coefficient, $\beta_L.a_e$, for Pall Ring Metal 25mm was selected. After that, the calculated value for volumetric mass transfer coefficient, $\beta_L.a_e$, for Pall Ring Metal 25mm was taken from Figure 35 based on the experimental value selected in Figure 34.

Table 10: Experimental and calculated value of $\beta_L.a_e$ for Pall Ring Metal 25mm

U_L (m/s)	0.00285
Experimental $\beta_L.a_e$ Value (1/s)	0.01
Calculated $\beta_L.a_e$ Value (1/s)	0.009

In order to determine which formula for volumetric mass transfer coefficient, $\beta_L.a_e$, to be used, the Reynold Number, Re_L, need to be determined.

$$Re_L = \frac{u_L}{a \cdot v_L} = \frac{0.00285 \, m \cdot s^{-1}}{232.1 m^{-1} \times \left(0.961 \times 10^{-6} \, m^2 \cdot s^{-1}\right)} = 12.778$$

Reynold Number is more than 2.0. Therefore, equation (14) is used to find the differential density, Δρ.

$$\beta_L \cdot a_e = 15.07194 \cdot \left[\frac{\Delta\rho^{1/2} \cdot g^{1/3} \cdot D_L^{1/2}}{(1-\varphi_P)^{1/3} \cdot d_h^{1/4} \cdot \sigma_L^{1/2}} \right] \cdot u_L^{5/6} \cdot a^{1/6}$$

Hydraulic diameter, d_h, was calculated using equation (12).

$$Hydraulic\ Diameter, d_h = \frac{4\varepsilon}{a} = \frac{4 \times 0.942}{232.1m^{-1}} = 0.0162\,m$$

After that, all the values and constants are substituted into equation (13).

$$0.009 = 15.07194 \cdot \left[\frac{\Delta\rho^{1/2} \cdot (9.81\,m \cdot s^{-2})^{1/3} \cdot (1.6 \times 10^{-9}\,m^2 \cdot s^{-1})^{1/2}}{(1-0.28)^{1/3} \cdot (0.0162\,m)^{1/4} \cdot (0.07275\,kg \cdot s^{-2})^{1/2}} \right] \cdot (0.00285\,m \cdot s^{-1})^{5/6} \cdot (232.1\,m^2)^{1/6}$$

$$0.009 = \left[\frac{\Delta\rho^{1/2} \cdot (1.290582 \times 10^{-3})}{0.086246} \right] \cdot (7.568980 \times 10^{-3}) \cdot (2.479015)$$

$$\Delta\rho^{1/2} = 32.053788$$

$$\Delta\rho = 1027.445\,kg \cdot m^{-3}$$

By having the constants for the system and for the packing elements, the performance for the new packing can be compared analytically using the mathematical model developed by Mackowiak (2011), Schultes (2011), and Higbie (1935). Figure 36 shows the effective interfacial area for mass transfer plotted against specific liquid load for mirv-1, VSP Ring Metal 50mm, Pall Ring Plastic 35mm, Pall Ring Metal 25mm, and Bialecki Ring Metal 12mm.
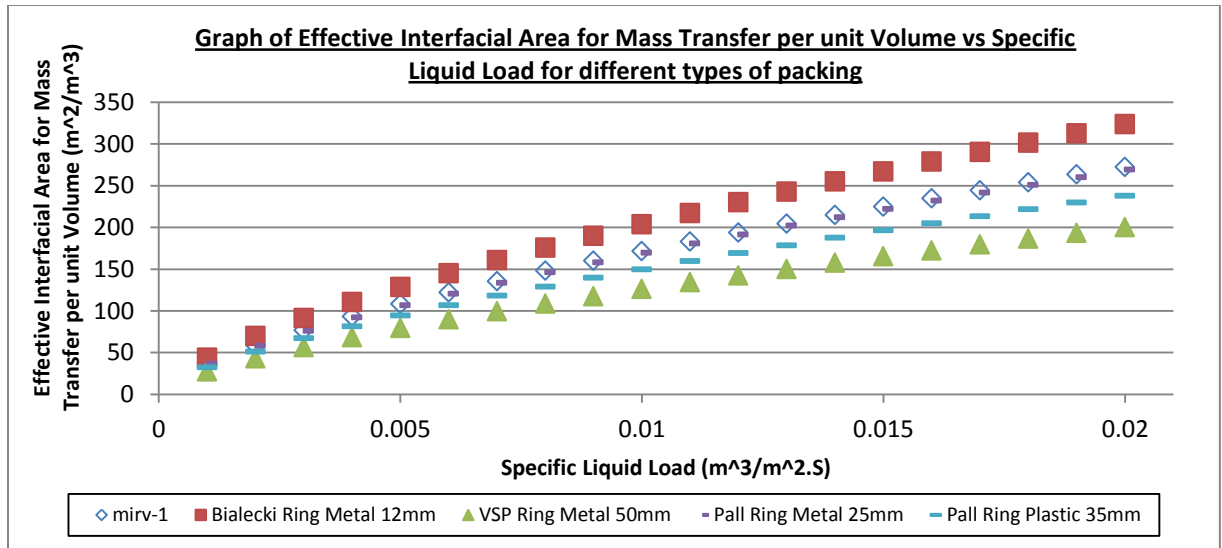
Figure 36: Graph of Effective Interfacial Area for Mass Transfer per unit Volume against Specific Liquid Load for different types of packing

The result in Figure 36 is calculated from equation (3), (5), and (7). According to equation (3), (5), and (7), effective interfacial area for mass transfer per unit volume is directly proportional to the geometric surface area of packing. Based on Figure 36, the effective interfacial area for mass transfer per cubic meter of packing for mirv-1 at varying specific liquid load is higher than VSP Ring Metal 50mm, Pall Ring Plastic 35mm, and Pall Ring Metal 25mm. This is because the geometric surface area of packing per cubic meter for mirv-1 is larger compared to the 3 packing elements. However, Bialecki Ring Metal 12mm still provides better effective interfacial area for mass transfer compared to mirv-1 because it has larger geometric surface area compared to mirv-1.

Figure 37 shows the liquid phase mass transfer coefficient plotted against specific liquid load for mirv-1, VSP Ring Metal 50mm, Pall Ring Plastic 35mm, Pall Ring Metal 25mm, and Bialecki Ring Metal 12mm.

Figure 37: Graph of Liquid Phase Mass Transfer Coefficient against Specific Liquid Load for different types of packing

The result in Figure 37 is calculated from the equation (5), (8), (11), (12), and (13). Based on Figure 37, the liquid phase mass transfer coefficient for mirv-1 is higher compared to VSP Ring Metal 50mm, Pall Ring Plastic 35mm, and Bialecki Ring Metal 12mm.

Figure 38 shows the volumetric mass transfer coefficient plotted against specific liquid load for mirv-1, VSP Ring Metal 50mm, Pall Ring Plastic 35mm, Pall Ring Metal 25mm, and Bialecki Ring Metal 12mm.
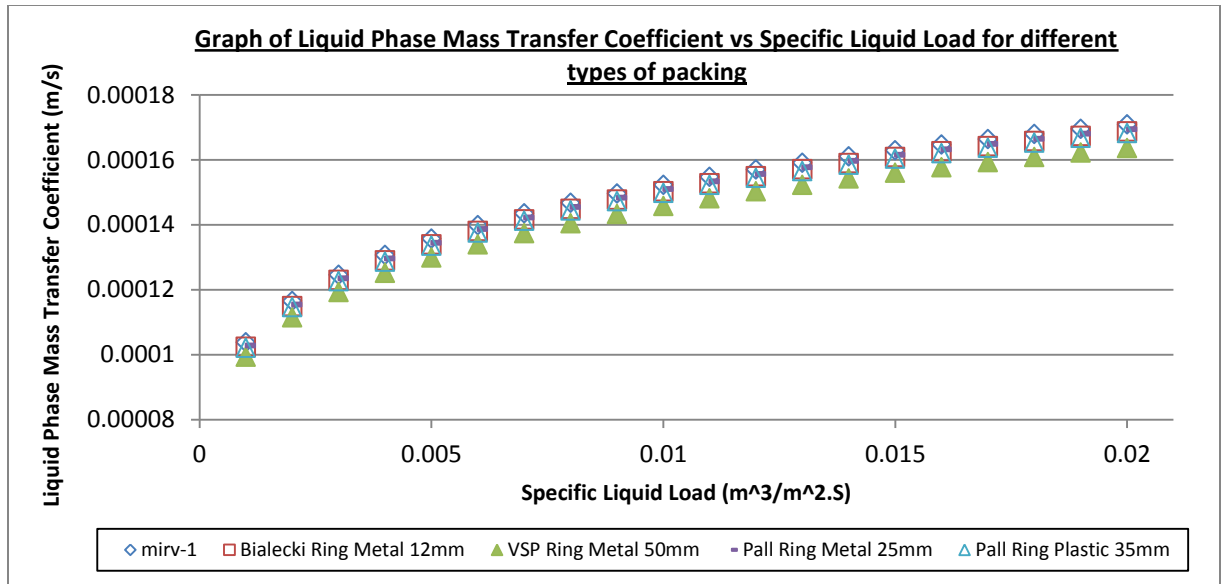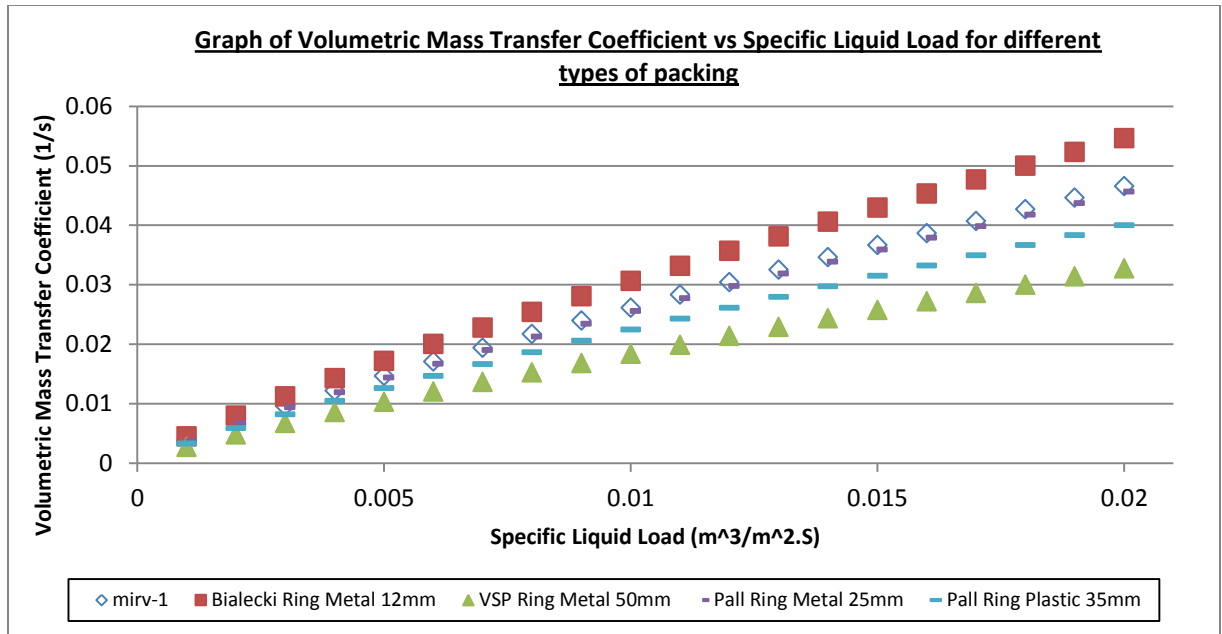
Figure 38: Graph of Volumetric Mass Transfer Coefficient vs Specific Liquid Load for different types of packing

The result in Figure 38 is calculated using the equation (14). According to equation (14), the volumetric mass transfer coefficient is proportional to the geometric surface area of packing. Based on Figure 38, the volumetric mass transfer coefficient for mirv-1 is higher compared to VSP Ring Metal 50mm, Pall Ring Plastic 35mm, and Bialecki Ring Metal 12mm. This is because the geometric surface area of packing per cubic meter for mirv-1 is larger compared to the 3 packing elements. According to equation (14), the effective interfacial area for mass transfer per unit volume is directly proportional to the geometric surface area of packing. However, Bialecki Ring Metal 12mm still provides better volumetric mass transfer coefficient compared to mirv-1 because it has larger geometric surface area compared to mirv-1.

4.5.2 Mass Transfer Experiment using an Air-Water Counter Current Flow

A series of experiments were conducted for mirv-1 to check whether the new packing element actually works. The experiments were conducted using the air-water countercurrent flow system as described in Chapter 3.

Figure 39 shows the mass transfer rate plotted against superficial gas velocity at varying specific liquid load.
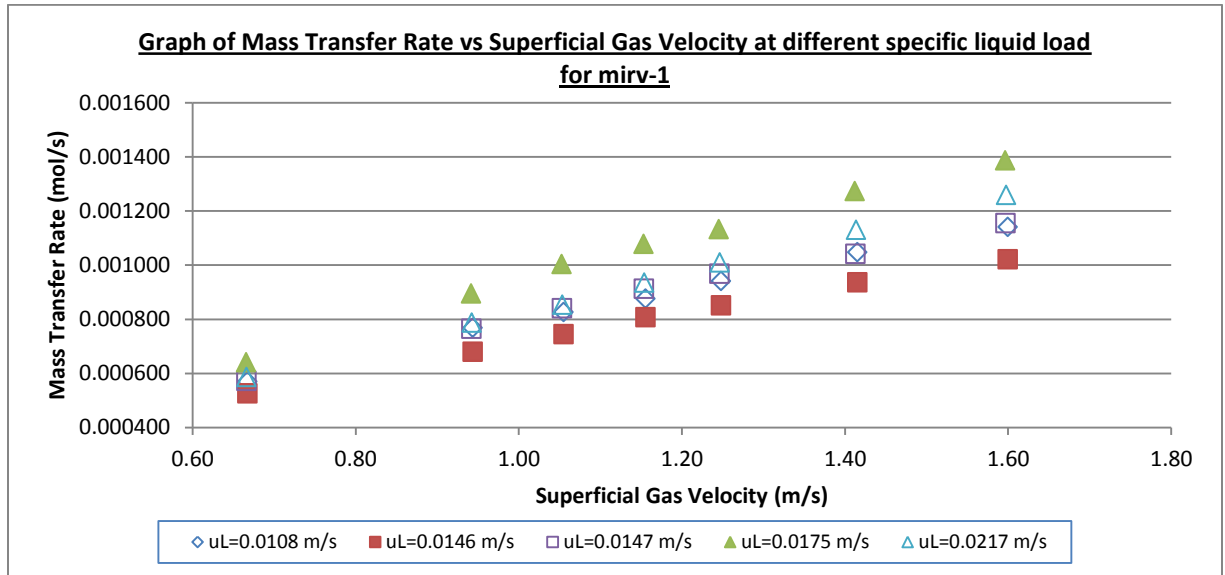

Figure 39: Graph of Mass Transfer Rate against Superficial Gas Velocity at different specific liquid load for mirv-1

Based on Figure 39, the mass transfer rate increases as the superficial gas velocity increases. This experimental result is the same as the expected result. However, the mass transfer rate shows inconsistency towards varying specific liquid load. The expected result is that the mass transfer rate will increase as the specific liquid load increases. This is because higher specific liquid load will increase the wetting efficiency of mirv-1, causing more mass transfer area to be available. As the mass transfer area increases, the mass transfer rate will also increase.
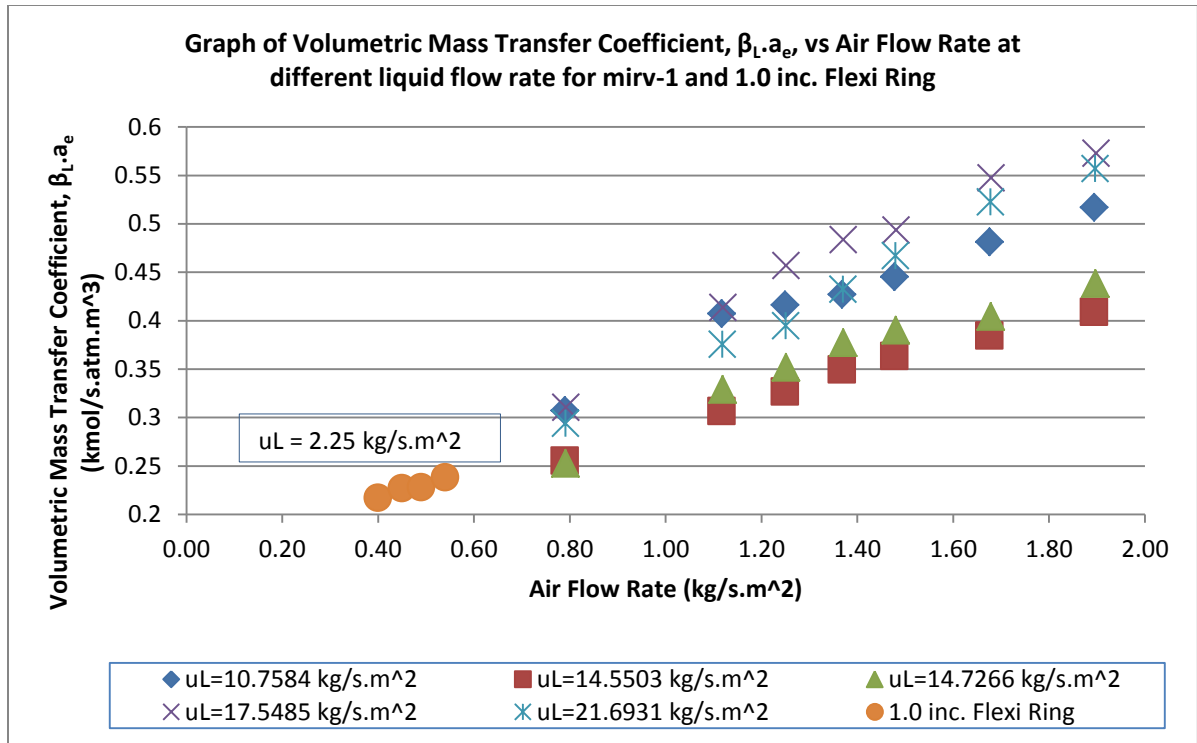
Figure 40: Graph of Volumetric Mass Transfer Coefficient against Air Flow Rate at different liquid flow rate for mirv-1 and 1.0 inch Flexi Ring

Based on Figure 40, the volumetric mass transfer coefficient, $\beta_L.a_e$, increases as the air flow rate increases. The experimental results behave as expected. However, volumetric mass transfer coefficient, $\beta_L.a_e$, shows inconsistency towards varying specific liquid load. The expected result is that the volumetric mass transfer coefficient, $\beta_L.a_e$, will increase as the specific liquid load increases. This is because higher specific liquid load will increase the wetting efficiency of mirv-1, causing the volumetric mass transfer coefficient, $\beta_L.a_e$, to increase. As the volumetric mass transfer coefficient, $\beta_L.a_e$, increases, the mass transfer rate will also increase.

The inconsistency is due to the way the experiment is conducted. Some of the test runs were conducted on different days. Compressed air was used in the experiment and the air is obtained from atmosphere. Since some of the test runs were conducted on different days, some of the days got rain. This will cause changes in humidity and affect the driving force for mass transfer.

Figure 40 also shows the volumetric mass transfer coefficient, $\beta_L.a_e$, against varying air flow rate at constant specific liquid load for 1.0 inch Flexi Ring. The result was based on the work of Wu and Chung (2009). They conducted the experiment using air-water countercurrent flow system. The mass transfer rate were calculated using wet bulb and dry bulb temperature of entering and exiting air passing through the absorber column.

Based on Figure 40, the 1.0 inch Flexi Ring gives better volumetric mass transfer coefficient, $\beta_L.a_e$, compared to mirv-1 eventhough the specific liquid load used for the 1.0 inch Flexi Ring is approximately 5 times smaller than the specific liquid load used for mirv-1.

Table 11: Packing Characteristics of mirv-1 and 1.0 inch Flexiring

Characteristics	mirv-1	1.0 inch Flexi Ring
Geometric surface area per unit volume (m^2/m^3)	240.6375	207
Void fraction, ε	0.972	0.94

mirv-1 was expected to perform better than 1.0 inch Flexi Ring because mirv-1 has higher geometric surface area per unit volume compared to the 1.0 inch Flexi Ring. The factors suspected to cause mirv-1 to underperform are:

- Poor construction of experimental setup
- Calibration error of the digital thermometer
- Water is not properly distributed upon the packing element
- Calculation error

Eventhough inconsistencies in result at varying specific liquid load exist, the fact that the system is able to run and provide expected result for mass transfer rate and volumetric mass transfer coefficient, $\beta_L.a_e$, at varying superficial gas velocity shows promising opportunities that the packing element and the absorber system can be further improved for future experiments.

CHAPTER 5

CONCLUSION AND RECOMMENDATION

As a conclusion, the new packing element, mirv-1, shows a promising result for future development. The previous generation packing elements were made of rigid structure, causing them to have high structural strength but low mass transfer area compared to the new generation packing elements. The new generation packing elements were made of flexible structure, causing them to have high mass transfer area but low structural strength.

mirv-1 is a combination of the previous generation and new generation packing element. By combining the rigid structure of the previous generation and the flexible structure of the new generation packing element, the drawback of both the previous and new generation of packing can be overcome while maintaining the advantages of both generation packing elements. These advantages make mirv-1 to be the first next generation packing element.

The packing characteristics of mirv-1 such as geometric surface area, void fractions, and equivalent spherical diameter of packing particle shows that mirv-1 is comparable with other packing elements used in the industry. Performance analysis using the stated equation and correlation also indicates that the performance of the new packing element is comparable with other existing packing elements. Besides that, experiments conducted on mirv-1 shows that the pressure drops and mass transfer performance of mirv-1 is within the acceptable range applied in the industry. Based on these results, it

can be concluded that mirv-1 has proven itself and worthy to be further develop to increase its performance.

Suggested future work for expansion of the project is to provide a better experimental setup to test the packing element. The experimental setup should be properly built and have sensitive and accurate measurement devices to measure mass transfer rate, pressure drop across packed bed, air flow rate, and liquid flow rate. Besides that, the setup should use better mass transfer system than air and water such as CO_2 and water system. The suggested experimental setup should give better and more accurate result for the mass transfer rate and pressure drop test.

REFERENCES

Schultes, M. (2003). RASCHIG SUPER-RING A New Fourth Generation Packing Offers New Advantages. Trans IChemE, Vol 81, Part A.

Mackowiak, J. (2011). Model for the prediction of liquid phase mass transfer of random packed columns for gas-liquid systems. CHEMICAL ENGINEERING RESEARCH AND DESIGN, 89 (2011), 1308-1320.

Subbarao, D., Rosli, F. A., Azmi, F. D., Manogaran, P., & Mahadzir, S. (2013). A Rivulet Flow Model For Wetting Efficiency In a Packed Bed. *AIChE Spring Meeting, San Antonio, Texas, U.S.A* .

Lee, K. R., & Hwang, S. T. (1989). GAS ABSORPTION WITH WETTED-WICK COLUMN. Korean J. of Chem. Eng., 6(3) (1989) 259-269.

ATCOM (Pty) Ltd. (2013). Retrieved June 18, 2013, from http://www.actomapc.co.za/images/packedtowers.jpg

Maćkowiak, J. (2010). *Fluid Dynamics of Packed Columns: Principles of the Fluid Dynamic Design of Columns for Gas/Liquid and Liquid/Liquid Systems*: Springer Berlin Heidelberg.

Kolev, N., Razkazova-Velkova, E., & Lozanov, P. (2004). A new principle for creation of packings operating at extremely low liquid superficial velocity. *Chemical Engineering and Processing: Process Intensification, 43*(1), 1-7. doi: http://dx.doi.org/10.1016/S0255-2701(02)00183-6

Kolev, Nikolai, & Razkazova-Velkova, Elena. (2001). A new column packing for operation at extremely low liquid loads. *Chemical Engineering and Processing: Process Intensification, 40*(5), 471-476. doi: http://dx.doi.org/10.1016/S0255-2701(00)00144-6

Geankoplis, C.J. (2003). *Transport Processes and Separation Process Principles: Includes Unit Operations*: Prentice Hall Professional Technical Reference.

Cheah, S.M. (2000). ABSORPTION. doi: http://www.separationprocesses.com/Absorption/MainSet2.htm

(n.d.). AceChemPack Tower Packing Co., Ltd. doi: http://www.tower-packing.com/Dir_column_packing.htm

(n.d.). Psychrometric Calculations. doi: http://www.sugartech.co.za/psychro/

(n.d.). Mass diffusivity. Wikipedia. doi: http://en.wikipedia.org/wiki/Mass_diffusivity

(n.d.). Air – Absolute and Kinematic Viscosity. The Engineering ToolBox. doi: http://www.engineeringtoolbox.com/air-absolute-kinematic-viscosity-d_601.html

(n.d.). Water – Dynamic and Kinematic Viscosity. The Engineering ToolBox. doi: http://www.engineeringtoolbox.com/water-dynamic-kinematic-viscosity-d_596.html

(n.d.). Water Properties. doi: people.ucsc.edu/~bkdaniel/WaterProperties.html

Wu, H. & Chung, T.W. (2009). MASS TRANSFER PERFORMANCE OF PACKED-BED AND SPRAY-BED ABSORBERS COMPARED BY SURFACE TENSION. Department of Chemical Engineering. Chung Yuan Christian University. Chung Li.

APPENDICES

Appendix 1: Example of calculation for equivalent spherical diameter of packing, D_P

By definition, the equivalent spherical diameter of an irregularly-shaped object is the diameter of a sphere of equivalent volume.

The volume of a sphere is calculated using the following formula:
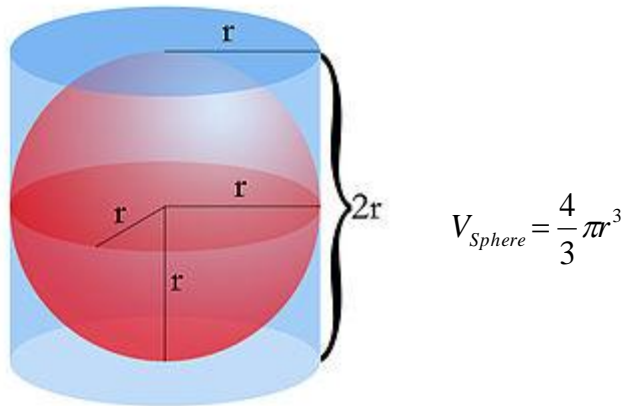
$$V_{Sphere} = \frac{4}{3}\pi r^3$$

The volume of a single flexible structure is $1.6806 \times 10^{-9} m^3$. Therefore, the equivalent spherical diameter of the packing is calculated as follows:

$$V_{Sphere} = \frac{4}{3}\pi r^3 = \frac{4}{3}\pi\left(\frac{D_P}{2}\right)^3 = \frac{4}{3}\pi\left(\frac{D_P^{\,3}}{8}\right) = \frac{\pi D_P^{\,3}}{6} = 1.6806 \times 10^{-9} m^3$$

$$D_P = \sqrt[3]{\frac{6\left(1.6806 \times 10^{-9} m^3\right)}{\pi}} = 0.001475\,m$$

Appendix 2: Example of orifice air flow meter calculation

Pipe diameter, D_i = 3.8 cm
Orifice diameter, D_o = 1.3 cm
Orifice pressure difference in water height = 0.2 cm
Flow coefficient, C_f = 0.7
Inlet air Dry-bulb temperature = 22.3°C
Inlet air Wet-bulb temperature = 11.4°C
Density of Water = 1000.0 kg/m³

Based on equation (23), the orifice pressure difference is:

$$\Delta p = \rho g h = (1000.0\,kg/m^3) \cdot (9.81\,m/s^2) \cdot (0.002\,m) = 19.62\,kg/m \cdot s^2 = 19.62\,Pa$$

The area of the orifice, A_o, is:

$$A_o = \pi r^2 = \pi \frac{(0.013\,m)^2}{4} = 0.000133\,m^2$$

Based on the dry-bulb and wet-bulb temperature of the inlet air, the density of inlet air can be found in the psychometric chart.

ρ_{air} = 1.188 kg/m³

Substituting all the constants into equation (21), the volumetric flow rate of air can be calculated:

$$Q_{volume} = C_f A_O \sqrt{\frac{2\Delta p}{\rho}} = (0.7) \cdot (0.000133\,m^2) \cdot \sqrt{\frac{2(19.62\,kg/m.s^2)}{1.188\,kg/m^3}} = 0.000534\,m^3/s$$

The mass flow rate can be calculated by multiplying the volumetric flow rate with density:

$$Q_{mass} = (0.000534\,m^3/s)(1.188\,kg/m^3) = 0.0006344\,kg/s$$

The superficial gas velocity with respect to column cross-sectional area is calculated by dividing volumetric flow rate with column cross-sectional area:

$$V_s = (0.000534\,m^3/s)/(0.001134\,m^2) = 0.471\,m/s$$

Appendix 3: Example of Ergun's Pressure Drop

Void fraction, $\varepsilon = 0.972$
Superficial Gas Velocity, $V_s = 0.67$ m/s
Air density, $\rho = 1.184$ kg/m^3
Air dynamic viscosity, $\mu = 0.00001938$ kg/m.s
Equivalent spherical diameter of packing, $D_P = 0.001475$ m
Length of packing in the column, $L = 0.37$ m

By assuming $k_1 = 150$ and $k_2 = 1.75$, rearrange Ergun's equation to get the pressure drop on the left-hand side of the equation:

$$\Delta p = \frac{150(1-\varepsilon)^2 \mu V_s L}{D_P^2 \varepsilon^3} + \frac{1.75 \rho V_s^2 L(1-\varepsilon)}{D_P \varepsilon^3} \qquad [kg/m.s]$$

Substitute the constants value into the equation to calculate the pressure drop in Pascal:

$$\Delta p = \frac{150(1-0.972)^2(0.00001938\,kg/m.s)(0.67\,m/s)(0.37m)}{(0.001475\,m)^2(0.972)^3} +$$

$$\frac{1.75(1.184\,kg/m^3)(0.67\,m/s)^2(0.37m)(1-0.972)}{(0.001475m)(0.972)^3}$$

$$= 0.2828 + 7.1139$$

$$= 7.3967\,kg/m.s = 7.3967\,Pa$$

Appendix 4: Example of calculation for Ergun's Constant

Pressure drop = 4.91 kg/m.s^2
Void fraction, ε = 0.972
Superficial Gas Velocity, V_s = 0.67 m/s
Air density, ρ = 1.184 kg/m^3
Air dynamic viscosity, μ = 0.00001938 kg/m.s
Equivalent spherical diameter of packing, D_P = 0.001475 m
Length of packing in the column, L = 0.37 m

The modified Ergun's equation is:

$$\frac{\Delta p}{L}\frac{D_P}{\rho V_s^2}\left(\frac{\varepsilon^3}{1-\varepsilon}\right)\left(\frac{D_P V_s \rho}{(1-\varepsilon)\mu}\right) = \left(\frac{D_P V_s \rho}{(1-\varepsilon)\mu}\right)k_2 + k_1$$

The value for k_1 is assumed to be 150.

The value for Y-axis is calculated as follows:

$$\frac{\Delta p}{L}\frac{D_P}{\rho V_s^2}\left(\frac{\varepsilon^3}{1-\varepsilon}\right)\left(\frac{D_P V_s \rho}{(1-\varepsilon)\mu}\right)$$

$$= \frac{4.91\,kg/m.s^2}{0.37\,m}\frac{0.001475\,m}{(1.184\,kg/m^3)(0.67\,m/s)^2}\left(\frac{0.972^3}{1-0.972}\right)\left(\frac{(0.001475\,m)(0.67\,m/s)(1.184\,kg/m^3)}{(1-0.972)(0.00001938\,kg/m.s)}\right)$$

$$= (0.0368)(32.7975)(2156.2878)$$

$$= 2602.5272$$

The value for X-axis is calculated as follows:

$$\left(\frac{D_P V_s \rho}{(1-\varepsilon)\mu}\right)$$

$$= \frac{(0.001475\,m)(0.67\,m/s)(1.184\,kg/m^3)}{(1-0.972)(0.00001938\,kg/m.s)}$$

$$= 2156.2878$$

Once all the values for X-axis and Y-axis have been calculated at specified superficial gas velocity, a graph of Y-axis vs X-axis is plotted for every specific liquid load. A liner trend line is drawn along the plotted points and the gradient value is recorded.

The gradient value represents the value for constant k_2.

Appendix 5: Example of calculation for mass transfer

Inlet humidity ratio, $H_{W, In}$ (kg H_2O/ kg Dry Air) = 0.00448
Outlet humidity ratio, $H_{W, Out}$ (kg H_2O/ kg Dry Air) = 0.01599
Inlet mass flow rate of air, $M_{Wet\ Air}$ (kg/s) = 0.000896
Inlet volumetric flow rate of air, $V_{Wet\ Air}$ (m^3/s) = 0.000757
Volume of column occupied by packing, V (m^3) = 0.00041968

The inlet mass flow rate of air is for wet air. In order to get the mass flow rate of dry air, the following formula is applied:

$M_{Wet\ Air} = M_{H2O} + M_{Dry\ Air}$

$\qquad = (H_{W, In} . M_{Dry\ Air}) + M_{Dry\ Air}$

$\qquad = M_{Dry\ Air} (1+ H_{W, In})$

$M_{Dry\ Air} = M_{Wet\ Air} / (1+ H_{W, In})$

$\qquad = (0.000896\ kg/s)/ (1 + 0.00448) = 0.000892$ kg Dry Air /s

By having the value of dry air mass flow rate, the rate of mass transfer of water into air can be calculated:

Rate of mass transfer, $N_A = (H_{W, Out} - H_{W, In}) * M_{Dry\ Air}$

$$= (0.01599 - 0.00448) * 0.000892$$

$$= 0.000010267 kg\ H_2O\ /s$$

The rate of mass transfer in terms of mole can be calculated by dividing the calculated mass transfer with molecular weight of water:

Rate of mass transfer, N_A = [(0.000010267kg H_2O /s)/ (18.015 kg/kmol H_2O)]*1000

$$= 0.00057\ mol\ H_2O\ /s$$

$$= 0.00000057\ kmol\ H_2O\ /s$$

Appendix 6: Example of calculation for volumetric mass transfer, $\beta_L.a_e$

Based on equation (2), the rate of mass transfer is described as follows:

$$\eta_A = k_C.A.\Delta C_A = \beta_L.a_e.V.\Delta C_A \qquad [kmol\,s^{-1}]$$

According to Geankoplis (2003), the driving force for the mass transfer is the difference of vapor pressure of water and vapor pressure of water vapor in air. Therefore, the modified equation is

$$\eta_A = \beta_L.a_e.V.\Delta C_A = \beta_L.a_e.V.(P_V - P_{avg}) \qquad [kmol\,s^{-1}]$$

P_V and P_{avg} is expressed in terms of atm. Rearranging the equation will give the formula to calculate volumetric mass transfer coefficient, $\beta_L.a_e$.

$$\beta_L.a_e = \frac{\eta_A}{V.(P_V - P_{avg})} \qquad [kmol/m^3 \cdot s \cdot atm]$$

The steps and calculation of finding the volumetric mass transfer coefficient, $\beta_L.a_e$, are as follows;

Average temperature of water during the experiments is 25.0°C.

Saturated Vapor Pressure, Density for Water

Temp (°C)	Temp (°F)	Saturated Vapor Pressure (mmHg)	Saturated Vapor Density (gm/m³)	Temp (°C)	Temp (°F)	Saturated Vapor Pressure (mmHg)	Saturated Vapor Density (gm/m³)
-10	14	2.15	2.36	40	104	55.3	51.1
0	32	4.58	4.85	60	140	149.4	130.5
5	41	6.54	6.8	80	176	355.1	293.8
10	50	9.21	9.4	95	203	634	505
11	51.8	9.84	10.01	96	205	658	523
12	53.6	10.52	10.66	97	207	682	541
13	55.4	11.23	11.35	98	208	707	560
14	57.2	11.99	12.07	99	210	733	579
15	59	12.79	12.83	100	212	760	598
20	68	17.54	17.3	101	214	788	618
25	77	23.76	23	110	230	1074.6	...
30	86	31.8	30.4	120	248	1489	...
37	98.6	47.07	44	200	392	11659	7840

Saturated vapor pressure = 23.76 mmHg

Appendix 6: Continued

$P_V = \rho g h = (13534\ \text{kg/m}^3)*(9.81\text{m/s}^2)*(0.02376\ \text{m}) = 3154.581\ \text{Pa} = 0.03113\ \text{atm}$

The vapor pressure of water vapor in air is calculated using Antoine's equation. Using Antoine's equation;

$$\log_{10} P_{V,in} = A - \frac{B}{C+T}$$

For temperature of water between 0.0°C and 100.0°C, A=8.07131, B=1730.63, and C=233.426

$T_{inlet} = 23.1°C$

$$\log_{10} P_{V,in} = 8.07131 - \frac{1730.63}{233.426+T} = 8.07131 - \frac{1730.63}{233.426+23.1} = 1.3249$$

$P_{V,in} = 10^{1.3249} = 21.13\ mmHg$

$P_{V,\ in} = \rho g h = (13534\ \text{kg/m}^3)*(9.81\text{m/s}^2)*(0.02113\ \text{m}) = 2805.399\ \text{Pa} = 0.02769\ \text{atm}$

$T_{outlet} = 21.9°C$

$$\log_{10} P_{V,in} = 8.07131 - \frac{1730.63}{233.426+T} = 8.07131 - \frac{1730.63}{233.426+21.9} = 1.2932$$

$P_{V,in} = 10^{1.2932} = 19.6426\ mmHg$

$P_{V,\ in} = \rho g h = (13534\ \text{kg/m}^3)*(9.81\text{m/s}^2)*(0.0196426\ \text{m}) = 2579.1617\ \text{Pa} = 0.02545\ \text{atm}$

Therefore, $P_{avg} = \dfrac{P_{V,in} + P_{V,out}}{2} = \dfrac{0.02545 + 0.02657}{2} = 0.02657\ atm$

Based on the calculation earlier, $N_A = 0.00000057\ \text{kmol } H_2O\ /s$

Appendix 6: Continued

Therefore, the volumetric mass transfer coefficient, $\beta_L.a_e$, is calculated as follows;

$$\beta_L.a_e = \frac{\eta_A}{V.(P_V - P_{avg})} = \frac{0.00000057\,kmol/s}{(0.00042\,m^3)(0.00456\,atm)} = 0.2976\,kmol/m^3 \cdot s \cdot atm$$